

# Fermi Statistics of Weakly Excited Granular Materials in a Vibrating Bed I: Molecular Dynamics Simulations

Paul V. Quinn <sup>\*</sup> and Daniel C. Hong <sup>†</sup>

*Department of Physics, Lewis Laboratory, Lehigh University, Bethlehem, Pennsylvania 18015*

(December 2, 2024)

## Abstract

Molecular Dynamics simulations were carried out to test the thermodynamic theory of weakly excited, two-dimensional, granular systems [Hayakawa and Hong, Phys. Rev. Lett. **78**, 2764(1997)], where granular materials are viewed as a collection of spinless Fermions. We first determine the global temperature  $T$  by fitting the steady state density profile to the Fermi distribution function, and then measure the center of mass,  $\langle z(T) \rangle$ , and its fluctuations,  $\langle (\Delta z(T))^2 \rangle$  as a function of  $T$ . We find a fairly good agreement between theory and simulations, in particular, in the estimation of the temperature and the scaling behavior of  $\langle z(T) \rangle$  and  $\langle (\Delta z(T))^2 \rangle$ .

PACS numbers: 81.05 Rm, 05., 07.05Tp, 82.20.wt

## I. Introduction

In a recent paper, Hayakawa and Hong(HH) [1] explored a simple consequence of the excluded volume effect for a dense granular system. They proposed a thermodynamic theory

---

<sup>\*</sup>E-mail address: [pvq2@lehigh.edu](mailto:pvq2@lehigh.edu)

<sup>†</sup>E-mail address: [dh09@lehigh.edu](mailto:dh09@lehigh.edu)

for weakly excited, dissipative, nonequilibrium, granular systems from the view point of the elementary excitation of non-interacting spinless Fermions. Based on a simple thermodynamic argument and combined with the observation that the granular state in a vibrating bed may be viewed as an excited state, HH demonstrated that the steady state density profile must be given by the Fermi distribution function. This enables one to associate and define a macroscopic, global parameter,  $T$ , which is suitable to characterize the state of the vibrating system. The parameter  $T$  is the thermodynamic temperature, and its relation to external control parameters has been derived in ref.[1]. The theory of Hayakawa and Hong has been successful in explaining the observed density profile of the experimental data of Clement and Rajchenbach [2]. The purpose of this paper is to further test the predictions of HH using Molecular Dynamics simulations, in particular, with regards to the configurational statistics of granular materials in a vibrating bed. From the outset, it is important to mention that it is too much to try to do a precise comparison between the theory and simulations. This is because there are too many parameters in the MD codes, most notably, the spring constants along the normal and shear directions of contact affecting the collisional dynamics of the granular material. (For example, the bouncing velocity of the grain weakly depends on the mass of the grain for the soft hard sphere that can be deformed upon contact. For more details on this aspect, see section V.) Nevertheless, the comparison between the measured temperature  $T$  and the theoretical prediction is fairly good. Furthermore, the scaling aspects of the Fermi statistics predicted by the theory [1] seem to survive in the MD simulations. However, the proportionality constant or amplitude displays some discrepancy. For details, see section IV. This paper is organized as follows: we first explain the background of the thermodynamic theory in section II along with a summary of the theory of ref.[1] in section III. We then present the simulation results in section IV. In section V, is a discussion of some of the important issues related to this work.

## II. Background of Fermi Statistics and Thermodynamic Theory of Granular

## Materials

In order to convey the essential idea and avoid unnecessary confusion that may arise in invoking the language of quantum mechanics, we first explain the mathematical analogy between granular systems and quantum mechanical Fermi systems in simple terms using the following example of parking [3]. Suppose we want to accommodate 10 cars in a lot of 1,000 parking spaces. In this case, the excluded volume interaction among cars is essentially insignificant because the mean free path is large and consequently the probability of collisions will be small. Thus, cars can be essentially treated as point particles, and the statistics of cars in the parking lot essentially obey the Boltzmann statistics. This corresponds to the limit of strong excitation in granular materials where the mean free path of grains is large, and all the particles are essentially dynamically active.

Consider now an opposite limit where about 900 cars are competing for the 1,000 parking spaces. In this case, the excluded volume interaction becomes increasingly important because one can only park one car in each parking space. Similarly, grains in the dense regime can no longer be treated as point particles and the size of the grain must enter the theory. In this case, the proper kinetic equation is not the Boltzmann equation, but rather the Enskoq equation which takes into account the size of grains as well as their correlations. Furthermore, in dealing with grains, one must also recognize the role of gravity, because when the strength of the excitation is reduced, a large fraction of particles becomes locked, rendering them dynamically *inactive*. Therfore, only a portion of grains near the surface participate in the dynamics.

This excluded volume interaction combined with the ordering of potential energy by gravity will manifest itself as what we term 'Fermi statistics'. The top surface of the granules plays the role of a Fermi surface, and the thin boundary layers that appear near the top layer upon excitations play the role of excited electrons in the Fermi gas in metals.

Now, the system being studied here is a dense, dissipative, nonequilibrium, granular system, where the mean free path of the grains is of the order of a few particle diameters.

Hence, each particle may be considered to be effectively confined in a cage as in the free volume theory of a dense liquid [4]. In such a case, an observation has been made in ref.[1] that the basic granular state is not a gas, but a solid or crystal, and thus the effective thermodynamic theory based on the free energy argument may be more appropriate than the kinetic theory in studying this state. In such a case, the *configurational* statistics of the steady state may be determined by the variational method as the most probable or minimum free energy state.

To be more specific, consider the excitation of disordered granular materials confined in a box with vibrations of the bottom plate. The vibrations will inject energy into the system which cause the ground state to become unstable, and a newly excited state will emerge with an expanded volume. The time averaged configurational states of this new excited state have undergone structural distortions. However, the degree of distortions from the ground state may be small for a weakly excited state, possibly justifying the use of an effective thermodynamic theory based on the variational principle. Such a thermodynamic approach may be further justified by the following two recent experiments:

1. Weakly or moderately excited regime: Clement and Rajchenbach(CR) [2] have performed an experiment with the vibrational strength,  $\Gamma$ , of the order one for a two dimensional vibrating bed, using inclined side walls to suppress convective flows. Here,  $\Gamma = A\omega^2/g$  with  $A$  and  $\omega$ , the amplitude and frequency of the vibrating plane, and  $g$ , the gravitational constant. CR have found that the ensemble-averaged density profile as a function of height from the bottom layer obeys a universal function that is *independent* of the phase of oscillations of the vibrating plate. Namely, it is independent of the kinetics imposed on the system. One conceptually important point here is that the reference point of the density profile is not the bottom plate, but the bottom layer, which of course is fluidized.

2. Highly excited regime: Warr and Hansen(WH) [5] have performed an experiment on highly agitated, vertically vibrating beds of  $\Gamma \approx 30 - 50$  using steel balls with a small coefficient of restitution. They have found that the collective behaviors of this vibrated

granular medium *in a stationary nonequilibrium state* exhibits strong similarities to those in an atomistic fluid in *thermal equilibrium* at the corresponding particle packing fraction, in particular, in the two-point correlation function [6].

The results of both experiments indicate that for both moderate or highly excited systems, one-to-one correspondence seems to exist between *configurational* statistics of nonequilibrium stationary state and the equilibrium thermal state. In fact, this is not so surprising considering that upon vibration, the granular materials expand and increase the volume of the system. In turn, this increase corresponds to a rise in the potential energy after the configurational average is appropriately taken. (For example, if a single ball is fired upward with the speed  $v_o$ , then the configurational statistics of such a ball is given by its average position,  $\langle z \rangle$ , defined as  $\langle z \rangle = \int_0^\tau z(t)dt/\tau = v_o^2/6g$  with  $z(t) = v_o t - gt^2/2$  and the period  $\tau = v_o/g$ .) Then the problem reduces to the packing problem, and the temperature-like variable,  $T$ , can be associated to the vibrating bed. The existence of distinctive configurational statistics in the density profile of CR (and also in WH in a special case) appears to be fairly convincing evidence that kinetic aspects of the excited granular materials may be separated out from the statistical configurations. These observations are the basis of the thermodynamic theory proposed in [1]. In this framework, one may employ the method developed in equilibrium statistical mechanics to characterize some of the properties of the excited granular materials, notably from the view point of elementary excitations such as Landau's Fermi liquid theory in condensed matter physics. The theory may also be extended to study the collective dynamics of granular materials, such as the problem of surface fluidization and granular compaction.

### III. Thermodynamic Theory of Weakly Excited Granular Systems

This part is a summary of ref.[1]. The starting point of ref. [1] is the recognition that a system of granular particles may be viewed as a mixture of holes and particles as it is in the lattice gas or the diffusing void model[7]. This is a discrete version of the stochastic

model of Litwiniszyn [8] and Mullins [8] as well as the simplest version of the free volume theory [4]. Here, a lattice model is used with the lattice spacing given by the diameter of a grain. In the presence of gravity, each row is given an energy level,  $\epsilon_i = mgD(i - 1/2)$ , with  $i$  being the integer that specifies the energy level. Each energy level has a degeneracy,  $\Omega = L/D$ , with  $L$  being the horizontal length of the box. When the box is not subject to vibrations, grains occupy the ground state, and a global temperature  $T=0$  is associated to it. Now, upon excitation, kinetic energy is injected into the system and the grains become excited, causing the time average position of each grain to increase as in the case of a single ball fired upward. Suppose there are  $N_i$  particles in the  $i$ -th energy level, and let the total number of particles be  $N$ , i.e,  $N = \sum_i N_i$ . Then, the total number of ways,  $W$ , of assigning positions to these  $N$  particles in the box is given by

$$W = \Pi W_i = \Pi[\Omega!/N_i!(\Omega - N)!], \quad (1a)$$

where  $W_i = \Omega!/N_i!(\Omega - N)!$  is the number of ways of putting  $N_i$  particles in each energy level with degeneracy  $\Omega$ . Obviously,  $N_i \geq \Omega$  for all  $i$ . Next, the entropy of the system is given by  $S = \ln W$ , and we postulate that the configurational statistics are given by the state that maximizes the entropy of the system. Hence, we now maximize  $S$  with the constraints that characterize the system, namely, the fixed number of particles,  $N$ , and the mean steady state energy  $\langle U(T(\Gamma)) \rangle$ , which is constant for a given temperature:

$$\Sigma_i N_i = N, \quad \Sigma_i N_i \epsilon_i = U. \quad (1b)$$

It is then straightforward to show that the density profile  $\phi(z)$ , which is the average number of occupied cells at a given energy level, *should be* given by the Fermi distribution [1],

$$\phi(z) = 1/[1 + \exp(\beta(z - \mu))], \quad (2)$$

with the Fermi energy,  $\mu(T)$ , measured in units of  $D$  and  $\beta = mgD/T$ , where  $T$  is the temperature and  $m$  is the mass of a grain. For electron gases, the Fermi energy  $\mu$  is a function of temperature because the density of states is not constant. In this granular

system, the density of states is constant, and thus  $\mu(T) = \mu(T = 0) = \mu_o$  with  $\mu_o$  being the initial number of layers. Note that here we employed the microcanonical ensemble approach, but the same answer can be obtained by using the canonical ensemble approach and thereby, minimizing the free energy. In this case, the free energy can be written as a functional of the coarse grained local density,  $\phi(\mathbf{r})$ ;

$$F(\phi) = U - TS = m \int dz g\phi(z)z + T \int d\mathbf{r} (\phi \ln \phi + (1 - \phi) \ln (1 - \phi))$$

where the first term represents the gravitational energy and the second term represents the entropy of the grains and the holes. A variation of  $F$  with the constraint  $N = \int d\phi$  then yields the Fermi distribution, namely,  $\delta F/\delta\phi = \mu$  with  $\mu$  being the Lagrangian multiplier [9].

Note that strongly excited systems are in a gaseous state, and the mean free path is much larger than the particle diameter. In such cases, the exclusion principle plays no role, and the Fermi statistics do not apply. The breakdown of the Fermi statistics can be determined as follows. The energy injected per particle via vibration of the bottom plate is  $T_k = \frac{1}{2}mv^2 \approx \frac{1}{2}mA^2\omega^2$ . In a weak excitation limit, most excitations occur near the Fermi surface, allowing  $n_l$  layers to become fluidized. The potential energy required to achieve this fluidization per particle is of the order  $\Delta U = n_l mgD \approx \frac{1}{2}mA^2\omega^2$ . By equating this potential energy with the kinetic energy  $T_k$ , one can determine the thickness of the fluidized layer,  $n_l \approx \Gamma(A/2D)$  as a function of the vibrational strength. The Fermi statistics are valid when  $n_l$  is much smaller than the Fermi energy,  $\mu$ . For an electron gas, the Fermi energy is of order  $eV \approx 10^4 K$ . Hence, at room temperature this ratio is;  $n_l/\mu \approx 10^{-2}$ . For granular systems, the Fermi description will break down when the following inequality is violated:

$$\mu \gg \Gamma \bullet A/D. \quad (3)$$

The next step is to relate the temperature variable,  $T$ , to the external control parameters. To this end, an observation has been made in [1] that for weakly excited systems, most excitations occur near the Fermi surface. Thus, it is possible to equate  $U(T)$ , the thermal

expansion of the system energy, to the kinetic expansion of the system. Both cases are considered separately.

**The Kinetic Expansion:** First, the system is examined from a mechanical point of view. The system actually undergoes mechanical vibration, receiving energy from the vibrating bottom layer, and transferring it throughout the system via inelastic collisions. Consequently, the system will expand. This expansion is due to the kinetics imposed on the system, and the precise amount of the expansion may be computed using a kinetic theory that includes dissipation. Considering the mathematical complexity involved in such an approach, however, an approximate method is called for in computing this kinetic expansion. Since most excitations occur near the Fermi surface, an assumption was made in ref.[1] that the kinetic expansion may be approximated by the motion of a single ball jump at the Fermi surface undergoing the same vibration as the bottom plate. In making this assumption, the lattice picture, where most particles below the Fermi surface are locked in their positions, is kept in mind. This is not quite true in the continuum case where particles below the Fermi surface do have room to shuffle around. In this paper, two different methods were used to obtain the single ball jump height  $h_o(\Gamma)$ .

(a) The first method is based on the theoretical examination of a particle gently launched from a vibrating plate.[1,10] Let the position of the vibrating plate in the lab frame be  $S(t) = A\sin(\omega t)$ , and that of the ball be  $z(t)$ . The relative distance between the ball and the plate,  $\Delta(t)$ , is  $z(t) - S(t)$ . If the ball is launched at  $t_o$ , then  $\Delta(t_o) = 0$ . It may be assumed that a gently launched particle has a zero relative velocity at the time of launching, i.e.  $(d\Delta(t)/dt)_{t_o} = 0$ . In this case, the launching velocity of the ball,  $v_o$ , is the same as that of the plate, i.e.  $v_o = A\omega\cos(\omega t_o)$ . This, of course, is generally not true because the relative velocity can be fairly large if the ball and the plate are out of phase. Now, in order to determine  $t_o$ , it is further assumed that the gently launched particle has zero relative acceleration between the ball and the plate, i.e.  $(d^2\Delta/dt^2)_{t_o} = 0$ . In this case, the particle will take off from the plate solely due to inertia when the acceleration of the plate becomes

-g. Note that  $\Delta(t)$  between the ball and the plate is given by [1]

$$\begin{aligned}\Delta(\omega t) &= (g/\omega^2)[\Gamma[\sin(\omega t_o) - \sin(\omega t)] + \Gamma \cos(\omega t_o)(\omega t - \omega t_o) - \frac{1}{2}(\omega t - \omega t_o)^2] \\ &\equiv (g/\omega^2)h_o(t, \Gamma),\end{aligned}\quad (4)$$

where  $\omega t_o = \sin^{-1}(1/\Gamma)$ . The maximum of  $h_o(\Gamma)$  is only a function of  $\Gamma$  and will be denoted by  $H_o(\Gamma)$ . (It can be determined from eq.(4) by setting  $g = \omega = 1$ .) In Table I are the values of  $H_o(\Gamma)$  as a function of  $\Gamma$ .

(b) The previous method of approximating  $H_o(\Gamma)$  works for any vibration that is an analytic function with an analytic velocity function and non-uniform acceleration. However, with a triangular wave, a particle sitting at the bottom plate cannot obtain the necessary acceleration to take off because the wave exerts zero acceleration. In this case, particles must collide with the plate violently and the velocity and the acceleration at the time of collisions will depend both on the Molecular Dynamics code and the initial conditions. In such a case, it may be more appropriate to directly measure the single ball jumping height on a vibrating plate, and find its maximum, denoted as  $h_{o\max}(\Gamma)$ .  $h_{o\max}(\Gamma)$  will be different from  $gH_o(\Gamma)/\omega^2$  determined in (a) because the launching velocity of the ball at the plate is, on the average, substantially different from those considered in (a). The Molecular dynamics program used in this paper employed the Hertzian forces to model the impacts occurring between the particle and the plate.

**The Thermal Expansion:** Now, the system is examined from the thermodynamic point of view. The vibrating system is considered a thermally equilibrated system with regard to the *configurational* properties. In this case, the vibrating bed is replaced by a thermal reservoir at the temperature  $T$ , each particle receiving energy from the heat reservoir. This thermal energy is then converted into a rise in the average position of each particle through the exchange of its potential and kinetic energies. Thus, in the configurational statistics, the average position of the particle rises and the system expands. This expansion is now a thermal expansion. The magnitude of this thermal expansion is measured by monitoring the

*total* increase in the height [or equivalently the volume] of the system. More precisely, the total system energy,  $E$ , is given by  $E(T) = \sum_i \Omega \rho_i \epsilon_i = \Omega \sum_i mgD(i-1/2)/[1+\exp([mgD(i-1/2)\mu]/T)]$ . In the continuum limit, where  $D\Delta i \rightarrow \Delta z$ ,  $(i-1/2)D \rightarrow z$ , and  $\sum \bullet \Delta z \rightarrow \int dz$ , it reduces to  $E = \frac{\Omega}{mgD} \int_0^\infty \frac{\epsilon d\epsilon}{1+\exp((\epsilon-\bar{\mu})/T)} = \Omega M_1 / mgD$  with  $M_n = \int_0^\infty \frac{\epsilon^n d\epsilon}{1+\exp((\epsilon-\bar{\mu})/T)} = \frac{\mu^{n+1}}{n+1} [1 + \frac{\pi^2 n(n+1)}{6} (\frac{T}{\bar{\mu}})^2]$ . Separating out the units of the Fermi energy, one gets  $\bar{\mu} \rightarrow mgD\mu_o$  with  $\mu_o$  being the dimensionless number of layers of the Fermi surface. (Note in MD simulations in section IV,  $\mu = D\mu_o$ , because the temperature was divided by mg, i.e,  $T \rightarrow T/mg$ , and has the dimension of length.) The average total potential energy per column,  $\bar{u}$ , is then given by

$$\bar{u} = E/\Omega = mgD \frac{\mu_o^2}{2} [1 + \frac{\pi^2}{3} (T/mgD\mu_o)^2]. \quad (5a)$$

This energy increase results in an increase in the column height and thus, an increase in the total potential energy of the column. The total center of mass,  $h(T)$  is the sum of the center of masses of all the particles in the column. Hence, one can relate the total center of mass,  $h(T) = \mu_o z(T)$ , to the total energy per column with the relation  $\bar{u}(T) = mgh(T)$  to get

$$h(T) = \bar{u}/mg = \frac{D\mu_o^2}{2} [1 + \frac{\pi^2}{3} (T/mgD\mu_o)^2]. \quad (5b)$$

Here, the increment in the total center of mass,  $\Delta h(T)$ , is given by

$$\langle \Delta h(T) \rangle = \mu_o \Delta z(T) = \langle h(T) \rangle - h(0) = h(0) \frac{\pi^2}{3} \left( \frac{T}{mgD\mu_o} \right)^2 \quad (5c)$$

with  $h(0) = D\mu_o^2/2$ . Or in terms of the center of mass  $\langle z(T) \rangle = \langle h(T) \rangle / \mu_o$ ,

$$\langle \Delta z(T) \rangle = \frac{D\mu_o \pi^2}{6} \left( \frac{T}{mgD\mu_o} \right)^2 \quad (5d)$$

This is the thermal expansion. Note that the *total* volume expansion of the system,  $\Delta h \equiv \mu \Delta z$ , is independent of the Fermi energy (i.e the initial number of layers), but is only a function of the reservoir temperature  $T$ .

Now, by equating the thermal expansion,  $\Delta h$ , and kinetic expansion,  $g/\omega^2 H_o(\Gamma)$ , one finds the closure in the thermodynamic theory of powders. Since the density decrease above the Fermi surface is not sharp, but smooth, one may replace  $gH_o(\Gamma)/\omega^2$  with  $h(\Gamma)/\alpha$ , where

$h(\Gamma)$  is the actual jump height of the single ball at the Fermi surface determined by the two different methods in the kinetic expansion. The factor  $\alpha$  was introduced to incorporate (i) the smooth decrease in the density profile near the Fermi surface, and (ii) the suppression in the jump height due to dissipation. By equating the kinetic expansion and the thermal expansion (5c), one obtains the following explicit relationships between the temperature  $T$  and the control parameters:

$$\frac{T}{mg} = \frac{1}{\pi} \sqrt{\frac{6D(gH_o(\Gamma)/\omega^2)}{\alpha}} \quad (6a)$$

$$= \frac{1}{\pi} \sqrt{\frac{6Dh_{omax}(\Gamma)}{\alpha}}. \quad (6b)$$

Note that when a single particle is on a vibrating plate, the energy from the bottom wall is transferred to the particle through direct contact. In the case of many particles, the supplied energy at the vibrating plate must first travel through other particles locked in their respective lattice states before reaching those particles in the fluidized layer. For (6a),  $gH_o(\Gamma)/\omega^2$ , the maximum of the single ball jump height, is a lower bound because the relative velocity between the ball and the plate is assumed to be zero, making this temperature a lower limit for the system. In reality the relative velocity can be much higher and  $\alpha$  could be smaller than 1. For (6b), the expansion of the fluidized layer near the Fermi surface is certainly less than the simulated single ball jump height because of the dissipation of energies through collisions. In this case,  $\alpha$  is like a dissipation constant. The best fit  $\alpha$ 's used in this work were  $\alpha = 1$  in (6a) and  $\alpha = 64/5$  in (6b). The second value of  $\alpha$  fit all the data, regardless of whether the sine wave or the triangular wave was used to vibrate the bottom wall. With  $\alpha = 1$  in eq.(6a), we find the relation between the actual jump height of the single ball,  $h_{omax}$ , and that of the gently launched ball,  $h_{gentle} = gH_o(\Gamma)/\omega^2$ , i.e.,  $h_{omax} \approx h_{gentle} \bullet 64/5$ : the average jump height of the grain at the Fermi surface is about eleven times smaller than that of the single ball in the free surface. Certainly, a large amount of energy is dissipated inside the granular block as the energy transfers from the vibrating plate toward the Fermi surface.

**Fluctuations of the Center of Mass:** We now examine the fluctuations of the center of mass. In computing the ensemble average of these fluctuations, one should recall the relationship between the energy fluctuations and the specific heat,  $C_V$ . For a system with total energy  $U = \Omega\bar{u}$ , if the probability,  $P(U)$ , of finding such a system obeys the Boltzmann hypothesis,  $P(U) \propto \exp(-\beta U)$ , then the following relationship can be easily derived:  $\langle (\Delta U)^2 \rangle = \langle (U - \langle U \rangle)^2 \rangle = T^2 C_V = T^2 dU/dT$ . Note that this fluctuation formula holds for both  $\bar{u}$  as well as for  $U$ . Further, note that  $U$  is an *extensive* quantity that is proportional to  $\Omega$ , i.e;  $\langle (\Delta U)^2 \rangle = \Omega \langle (\Delta u)^2 \rangle \neq \Omega^2 \langle (\Delta u)^2 \rangle$ . The system considered here is a thermal system, so one would expect the probability distribution of the energy of the system to follow the Boltzmann distribution. Thus, the fluctuation relationship should hold. Since the average energy per column,  $\bar{u} \equiv \langle u_i(T) \rangle = mg\bar{h}(T) = mg\mu_o \langle z(T) \rangle$ , one finds from the fluctuation formula:  $\langle (\Delta \bar{u})^2 \rangle = T^2 d\bar{u}/dT$ , i.e;

$$\langle (\Delta h)^2 \rangle = \frac{\pi^2 D^2}{3} \left( \frac{T}{mgD} \right)^3$$

Or, in terms of  $\langle z \rangle = \langle h \rangle / \mu_o$ , we find:

$$\langle (\Delta z)^2 \rangle = \langle (z(T) - \langle z \rangle)^2 \rangle = \langle (\Delta h)^2 \rangle / \mu_o^2 = \frac{\pi^2}{3} \left( \frac{T}{mgD} \right)^3 \frac{D^2}{\mu_o^2}. \quad (7)$$

Note again that  $\langle (\Delta h)^2 \rangle / D^2 = \langle \mu_o (\Delta z)^2 \rangle / D^2$  is only a function of the dimensionless Fermi temperature  $T_f = T/mgD$ . Further, note that (7) is an indirect confirmation that the specific heat is linear in T as it is for the non-interacting Fermi gas.

#### IV. Test of Fermi Statistics

We have carried out extensive Molecular Dynamics simulations to test the thermodynamic theory of ref.[1] by specifically measuring the density profile, its center of mass and the fluctuations of the center of mass. The simulation results are compared with Eqs. (2),(5b),(6) and (7). The MD code used in this paper was provided by Jysoo Lee. It is identical to those used by HLRZ group in Germany [11]. In brief, the forces,  $\mathbf{F}$ , acting on

two colliding particles,  $i$  and  $j$ , consist of two terms,  $\mathbf{F} = F_n \hat{n} + F_s \hat{s}$ . Here, the normal force is given by:

$$F_n = K_n(r_i + r_j - |\hat{r}_i - \hat{r}_j|)^n \hat{n} - \gamma_n m_{eff} \hat{v} \bullet \hat{n}, \quad (8)$$

where  $K_n$  is the elastic spring constant or Young's modulus with the magnitude  $K_n = 10^8$  dyne/cm,  $r_i$  and  $r_j$  are the radii of the  $i$ th and  $j$ th particles, and  $\hat{n}$  is the unit normal vector in the direction of  $r_{ij} = r_i - r_j$ . The first term in (8) is the Hertzian contact force, similar to the spring force if  $n$  is set to  $3/2$  [12]. In this work, as was done by HLRZ group,  $n$  is set to one. The second term is the frictional force with the friction coefficient  $\gamma_n = 3.15 \bullet 10^3 \text{dyn/cm/sec}$ , the effective mass  $m_{eff}$ , and the relative velocity  $\hat{v}_{ij} = v_i - v_j$ .  $F_s$ , the shear force, is given by

$$F_s = -\text{sign}(\hat{v}_{ij} \bullet \hat{s}) \bullet \min(\gamma_s \hat{v}_{ij} \bullet \hat{s}, \mu_f |F_n|). \quad (9)$$

The parameter  $\gamma_s = 10^8 \text{dyn/cm/sec}$  is set so the shear force is mainly dominated by the Coulomb threshold condition,  $\mu_f F_n$ , where  $\mu_f = 0.2$  for particle-particle and particle-wall contacts [11].

It is important to briefly discuss the parameters used in this model and their affect on the results of the simulations. Values for these parameters cannot be set randomly or the results of the simulation will become unphysical in nature. The parameters  $K_n$  and  $\gamma_n$  are used to define the duration of a two particle collision,

$$t_c = \frac{\pi}{\omega_p},$$

where  $\omega_p$ , a constant with the units of frequency, is defined as

$$\omega_p = \sqrt{\frac{K_n}{m_{eff}} - \frac{\gamma_n^2}{2}}.$$

Because the simulations discussed in this paper used particles with the same mass, the effective mass,  $m_{eff}$ , is just  $m/2$ . Unphysical results will occur when the time between collisions becomes smaller than  $t_c$ .

With the wrong set of parameters, unphysical results were indeed observed. For example, with the values of the normal parameters  $K_n = 10^5$  and  $\gamma_n = 10^3$ , the expansion of the center of mass as well as the fluctuations were increasing as the number of layers in our simulation increased. This effect was examined more closely using one dimensional columns of particles ranging from 3 to 60 layers. The expansion of the center of mass and the fluctuations behaved normally until the column reached a height of about 8 particles. At this point the results became unphysical. A similar trend was observed by Stephen Luding in his thesis work involving Molecular Dynamics simulations [11]. Such unphysical results began when the frequency of collisions became larger than  $1/t_c$ . Fluctuations of the center of mass increase as a result, leading to the observed increase in the expansion of the center of mass. This is called the detachment effect and is more prominent in simulations undergoing low frequency vibrations. More details on the detachment effect can be found in references [10]. To eliminate the detachment effect, it was necessary to decrease the collision time,  $t_c$ , leading to the larger values of  $K_n$  and  $\gamma_n$  reported above. With these values, the one dimensional column of particles did not yield any unphysical results until a height of over 55 layers was reached. None of the simulations used in this paper were over 50 layers high, so the results presented below have not been altered by the detachment effect.

It is important to emphasize that this MD code does not use hard spheres, but instead, allows the particles to deform. The elasticity of the particles,  $e$ , is given by the expression

$$e = \exp\left(-\frac{\gamma_n * t_c}{2}\right)$$

For the simulations presented in this paper,  $e \approx 0.8$ . The program was tested using a higher elasticity, but there were problems in setting up the initial configuration of particles. To start a simulation, the program first places the particles into a two-dimensional configuration specified in the code by the user. Then the particles are allowed to relax under gravity and the particle-particle and particle-wall interactions before any vibration is “turned on”. The vibration of the bottom plate should not begin until the particles are motionless. This relaxation time is found through trial and error while tracking the motion of the particles.

For a larger elasticity, the relaxation time becomes extremely large and not very practical to work with. Therefore the smaller elasticity was used for the completion of this project. Slight alterations of the MD code itself may lead to smaller relaxation times for larger elasticities, but as of yet this hypothesis is untested. Therefore, the results discussed in this paper are for soft spheres. It is not known whether hard sphere MD codes, [11] which do not allow particle deformations, will yield the same results. For more details on the MD code, see reference [11].

Using the MD code, the density profile was first measured and then fit with the Fermi distribution function. This allowed the determination of the temperature,  $T$ . The center of mass and its fluctuations were also measured by taking the average over the time sequences, namely,  $\langle h(T) \rangle = [\sum_{t=1}^{t_N} [(\sum_i^N z(i,t))/N]]/t_N]$  and  $\langle (\Delta h)^2 \rangle = [\sum_{t=1}^{t_N} [(\sum_i^N (z(i,t) - \langle z(i,t) \rangle)^2)/N]]/t_N]$ , where the average  $\langle h(T) \rangle$  is the configurational average at a given time and  $\langle (\Delta h)^2 \rangle$  is the average over time sequence,  $t_N$ . The configurational average was taken every 100 time steps, and  $t_N \approx 2 \bullet 10^7$ , which is approximately 2000 vibrating cycles. Then, the center of mass and the fluctuations are plotted as a function of time. We now present the data.

## 1. The Fermi Temperature $T$

Simulations were carried out in two dimensional boxes with vertical walls for  $N$  particles each with a diameter  $D = 0.2\text{cm}$  and a mass  $m = 4\pi(D/2)^3/3 = 4.188 \bullet 10^{-3}\text{gram}$  with degeneracy  $\Omega$  using  $(N,\Omega) = (100,4)$ ,  $(200,4)$ , and  $(200,8)$  with a sine wave vibration and  $(100,4)$  and  $(200,4)$  with a triangular wave. The dimensionless Fermi energy  $\mu_o = \mu/D = N/\Omega$ , which is the initial layer thickness, is  $\mu_o(N = 100) = 25$  for  $\Omega = 4$ ,  $\mu_o(N = 200) = 50$  for  $\Omega = 4$ , and  $\mu_o(N = 200) = 25$  for  $\Omega = 8$ . For all cases, the inequality (3) is checked. (Note that the values of  $\mu$  listed in Tables II and III are not the values of the dimensionless quantity  $\mu_o$ . The density profiles in this paper were fit using a  $\mu$  value with units of length, and then were converted to the dimensionless values for their use in inequality (3).) The width,  $L$ , of the bed is slightly larger than  $\Omega$  times the particle diameter; i.e.  $L = \Omega D + \epsilon$

with  $D = 0.2\text{cm}$  and  $\epsilon/D \approx 0.05/0.2 = 0.25$ . Initially, the particles were arranged on a square lattice, and the frequency  $\omega$  was set to a fixed value,  $\omega = 2\pi f = 40\pi$ , which is the experimental value ( $f=20\text{Hz}$ ) used by Clement and Rajchenbach [3]. The strength of the vibration,  $\Gamma = A\omega^2/g$ , was varied by changing the amplitude,  $A$ , of the vibration. Initially,  $\Gamma$  was varied from 1.2 to 20 in the simulations with  $g = 981\text{cm/sec}^2$ . The density profile closely follows the Fermi profile for low  $\Gamma$ 's, but it crosses over to the Boltzmann distribution for higher  $\Gamma$ 's (Fig.1). Note that the deviation from the Fermi profile for large  $\Gamma$  is quite noticeable. The deviation of the  $\Gamma = 20$  data from the Boltzmann function near the bottom plate is due to the model used to approximate particle-particle reactions in the simulation program. The springs used in the soft sphere model of these particles cause the odd motion observed in the bottom layers of the columns of particles. These bottom particles have more of a spring force than the top layers because the extra mass on top causes the bottom particles to deform more. This deformation leads to the separation of these bottom particles from the bulk, giving the density profile its odd shape from  $0 < z \leq 4$  for  $\Gamma = 20$ . Hence, our analysis is focused strictly for  $\Gamma \leq 4$ .  $A/D$  changes from 0.373 for  $\Gamma = 1.2$  to 1.24 for  $\Gamma = 4$ . For all the data,  $4.90 \leq R = \mu D/\Gamma A < 111.20$ , and thus, the inequality (3) is satisfied.

The sine wave simulation data for the density profile with  $(N,\Omega)=(100,4)$  for  $\Gamma = 1.2, 1.5, 2.0, 2.5, 3.0, 3.5$  and 4.0 is plotted in Fig.2a. Both sets of sine wave data for  $N=200$  with the same set of  $\Gamma$ 's are plotted in Fig.2b and Fig.2c. The sine wave data for  $(\Gamma, N, \Omega) = (2.0, 100, 4)$  [Fig.2d],  $(\Gamma, N, \Omega) = (2.0, 200, 4)$  [Fig.2e], and  $(\Gamma, N, \Omega) = (2.0, 200, 8)$  [Fig.2f] has been singled out to show the degree of accuracy obtained by using the Fermi fitting. (Note that the temperature,  $T_f$ , discussed in the following text is actually  $T/mg$ . This is because the fitting function  $\rho(z) = \rho_c/(1 + \exp[(z - \mu)/T_f])$  (See eq.(2)) was used with  $\mu = \mu_o D$  and  $z = (i - 1/2)D$  the height with units of centimeters.) The ratio  $R = \mu_o D/\Gamma A$  changes from 55.45( $\Gamma = 1.2$ ) to 5.25( $\Gamma = 4.0$ ) for  $N=100$  and  $\Omega = 4$  and from 52.05( $\Gamma = 1.2$ ) to 4.90( $\Gamma = 4.0$ ) for  $N=200$  and  $\Omega = 4$ . For  $N=200$  and  $\Omega = 4$ , this inequality is enhanced by a factor of  $\mu(200, \Omega = 4)/\mu(100, \Omega = 4) = 2$ . The triangular wave density profiles are not shown in this paper because they follow precisely the same trend with slightly different

values of the fitting parameters.

In fitting the simulation data with the Fermi profile, there are essentially three parameters: the closed packed density,  $\rho_c$ , the Fermi energy,  $\mu$ , and the temperature,  $T$ . The parameter  $\rho_c$  is the value of the density at the flat region, which is fairly easy to determine. The value  $\mu$  shifts the density profile horizontally, and the temperature  $T$  basically controls the curvature near the Fermi energy. The exact value of  $\rho_c$  for the square lattice is  $\rho_c = \pi(D/2)^2/D^2 = \pi/4 = 0.785$ , but for the data presented here,  $\rho_c$  is slightly larger than 0.785. This is because the particles are deformed, signified by the substantial overlaps that occur between particles in the simulation. This deformation stems from the use of soft spheres with an elasticity of 0.80 instead of hard spheres.

The Fermi energy,  $\mu$ , is expected to remain constant if the density of the state is constant. However, in our simulations of  $N=100$ , it changes from 4.96 cm to 5.26 cm with a relative increase of about  $\Delta\mu/\mu = 0.06$ . The slight increase in the Fermi energy does not affect the scaling behavoir of the center of mass and its fluctuations, but has a noticeable effect on the amplitude. One can also notice that the value of  $\mu$  will drop every once in a while with increasing  $\Gamma$ . This is due to the collapse of the system into a more tightly packed configuration. As  $\Gamma$  is increased, the amplitude of the motion of the bottom plate becomes larger. When the value of the amplitude is large enough, it causes the particles in the simulation to move more, sometimes resulting in a particle configuration more dense than before. As shown in Fig.2a-2f, one finds that the fitting to the Fermi profile is excellent.

The fitting values for  $\rho_c$ ,  $\mu$  and  $T_f$  for three different sets of sine wave simulations,  $(N, \Omega) = (100, 4), (200, 4)$  and  $(200, 8)$  are listed in Table II. Fitting values for the two triangular wave simulations are listed in Table III. Now the temperature  $T_f$  obtained by the Fermi fitting can be compared to the theoretical prediction,  $T_o$ , given by the formulas (6). As shown in the Table IV, when  $H_o(\Gamma)$  is used for the sine wave data, the predicted values are slightly lower than the fitted ones. This is not surprising if one recalls that in computing  $H_o(\Gamma)$ , it was assumed that the relative velocity between the ball and the plate was zero. For the MD codes used in this paper, the particles bounce off of the plate with a non-zero relative

velocity. So these predicted values must be a lower bound for the temperature formula. If  $h_o max(\Gamma)$  with  $\alpha = 64/5$  is used in our temperature formula, the predicted values match extremely well with the measured ones. A reasonable agreement between the theory and the simulation is reached when one uses  $h_o max(\Gamma)$  for both the sine and triangular wave data. This agreement is fairly constant for all five simulated systems. Now we turn our attention to the study of the temperature scaling.

## 2. Study of temperature scaling

We now test the scaling relation predicted by eq.(6a) and (6b) between the temperature and control parameters such as frequency ( $\omega$ ), gravitational acceleration ( $g$ ), and particle diameter ( $D$ ).

(a) Frequency Dependence: The frequency of the sine wave was varied for fixed values of  $\Gamma = 2.0$ ,  $N=200$ , and  $\Omega = 4$ , over the range  $5 \leq \omega \leq 35$ . The temperature was found to scale with frequency as

$$T \approx \omega^{m_1}$$

where  $m \approx 1.16$ , which is fairly close to the predicted value  $m_1 = 1$ . (Fig.3a)

(b) Gravity Dependence: Temperature as a function of the gravitational acceleration is displayed in Fig.3b with fixed values of  $\Gamma = 2.0$ ,  $N=200$ ,  $\Omega = 4$ , and  $f = \omega/2\pi = 20Hz$  for the range of  $150 \leq g \leq 1200$ . The temperature scales as

$$T \approx g^{-m_2}$$

where  $m_2 \approx 0.48$ , which is again, close to the predicted value  $m_2 = 0.5$ . We notice a change in the temperature dependence for  $g_c \geq g$  with  $g_c \approx 1000cm/sec^2$ , the reason for which is not so clear at this point.

(c) Diameter Dependence: The temperature as a function of the diameter,  $D$ , at the fixed frequency  $f = \omega/2\pi = 20Hz$  and  $g = 981cm/sec^2$  is displayed in Fig.3c with fixed values of  $\Gamma = 2.0$ ,  $N=200$ , and  $\Omega = 4$  for the range  $0.025 \leq D \leq 1.60$ . Here, as the diameter was changed, the density was changed accordingly using  $\rho = (3/4\pi D^3)m$  to ensure that the

mass remained at a constant value of  $4.188 \times 10^{-3} gm$ . The temperature scales as

$$T \approx D^{-m_3}$$

where  $m_3 \approx 0.53$ , which is again, close to the predicted value for  $m_3 = 0.5$ .

To summarize, we find that the scaling relations between the temperature and  $\omega$ ,  $g$ , and  $D$  appear to be consistent with the theoretical predictions within the error bars. Our next task is to examine the scaling relations presented for the center of mass and its fluctuations.

### 3. Center of Mass

The center of mass is plotted in Fig. 4 as a function of  $T^2$  in a graph of seven different  $\Gamma$ 's for  $N=200$ ,  $\Omega = 4$  and  $\Omega = 8$ , and  $N=100$ ,  $\Omega = 4$  under a sine wave vibration and  $N=100$ ,  $\Omega = 4$  and  $N=200$ ,  $\Omega = 4$  under the triangle wave vibration. The solid line, a guide for the eye, seems to confirm the scaling predictions of the Fermi statistics as given by the formula (5b), namely

$$\Delta z \propto T^2.$$

However, there exists a large discrepancy in the amplitude,  $C$ . For  $N=200$  and  $\Omega = 4$ , the theory predicts that one should get from (5d)  $C = \pi^2/6\mu_o = \pi^2/6\mu \approx .16$  with  $\mu = D\mu_o$ , the actual height of the Fermi surface. The simulation results yield,  $C \approx 3.0$  for the sine wave and  $C \approx 5.6$  for the triangular wave, a difference of a factor 20 and greater when compared to with the theoretical prediction. This discrepancy has been traced in some detail using Mathematica, and it appears that the center of mass defined in (5b) is *extremely* sensitive to a slight change in the Fermi energy,  $\mu$ . For example, if the average  $\mu = 10.01$  is used for the  $N=200$ ,  $\Omega = 4$  sine wave data and the integral is computed with Mathematica, the plot of the center of mass values as a function of  $T^2$  yield a slope that *is* indeed 0.16, just as predicted by the Fermi analysis. However, if the experimentally determined  $\mu$  ranging from 9.91 to 10.13 is used and the center of mass is computed using Mathematica, the slope turns out to be 2.5. Hence, one can conclude that the temperature dependence of  $\mu$  causes the huge discrepancy observed in the *amplitude*. Note that when the density of states is independent of the energy, the Fermi energy must remain constant. Yet, in real simulations,

it changes for each value of  $\Gamma$ . Fortunately, this 5 % change in the Fermi temperature does not make a noticeable difference in the Fermi fitting as shown in Fig.2a-2d. Therefore, the temperature fitting is robust.

#### 4. Fluctuations of the Center of Mass

The fluctuations of the center of mass were also measured and plotted as a function of  $T^3$  for  $N=200$ ,  $\Omega = 4$  and  $\Omega = 8$  and  $N=100$ ,  $\Omega = 4$  under a sine wave vibration and  $N=200$ ,  $\Omega = 4$  and  $N=100$ ,  $\Omega = 4$  under a triangle wave vibration.(Fig.5) Once again, this confirms the validity of the Fermi statistics which imply that

$$\langle (\Delta z)^2 \rangle \propto T^3.$$

The proportionality constant, though, is a way off from the theoretical value,  $D\pi^2/3\mu^2 \approx 6.4 \bullet 10^{-3}$ . The actual slope is of the order 1. Considering the fact that the amplitude in the center of mass is off by a factor 10, one can expect the errors in the fluctuations to be larger, of the order  $10^2$ . This is again due to the sensitivity of the Fermi integral to  $\mu$ . A small change in  $\mu$  is magnified in the fluctuations,  $\langle (\Delta z^2) \rangle$ , resulting in the  $10^2$  factor difference. An additional source of discrepancy is due to the fact that the fluctuations of the center of mass are quite large in the vibrating bed, and *all* the particles down to the ones at the very bottom of the layer fluctuate in a *continuum* space. This is in contrast to the Fermi particles of a lattice model, where most of the particles below the Fermi surface are locked and are thus, *inactive*. Hence, while the average position of the grains appear to obey the Fermi distribution function quite well, its actual magnitude in the fluctuations may not. The surprise here, however, is that the temperature dependence of the fltuuations still appears to obey the  $T^3$  law of the Fermi statistics.

Now, we now summarize the main results of our investigation as follows. **First**, the configurational statistics of granular materials in a vibrating bed do obey the Fermi statistics of spinless particles for weakly excited systems as predicted by HH[1]. The temperature, determined by fitting the Fermi profile, can be used as the thermodynamic temperature of the

vibrating bed, and the temperature formula(Eq.6a and b), based on a single ball's motion near the Fermi surface, seems to fit the measured temperatures quite well. **Second**, the scaling relations of the temperature with control parameters such as particle diameter, gravity, and frequency also appear to obey the theoretical prediction of HH[1] fairly well. **Third**, while the scaling relations of the center of mass and its fluctuations also obey the Fermi statistics with respect to the temperature, there are discrepancies in the proportionality constant.

## V. Discussion

There are several issues that should be discussed in connection with the present work.

*First*, the temperature formula, eq.(6b), certainly needs to be modified and improved. Apart from the difficulty of computing the entropy directly as a function of  $\Gamma$ , one point should be brought out which has been overlooked in studies of a vibrating bed. It has been assumed that the increase in the center of mass is a monotonic function of the vibration strength, namely, that the more energy injected, the more the volume will expand. However, since the energy is injected by a *vibrating plate*, this is not necessarily true due to the appearance of *resonance* phenomena.

*Second*, the thermodynamic aspect of the theory presented in [1] should be investigated in more detail in the future. Note first the obvious fact that the temperature in the Fermi distribution function is not the same as the kinetic temperature,  $T_k = m < v^2 > /2$ .  $T_k$  is zero when there is no motion, but the temperature  $T$  defined in ref [1] is non zero even though there is no motion because of the entropic contribution. In this sense, our theory is similar to that proposed by Edwards [13]. Edwards and his collaborators proposed a thermodynamic model for an *equilibrium* state by defining a temperature like variable, termed the compactivity,

$$X = \frac{\partial V}{\partial S},$$

where  $V$  is the total volume of the granular system, and  $S$  is its entropy. The volume  $V$  can be determined easily, but there is no systematic way of determining the entropy,  $S$ , of a disordered system. Hence, there is no calculational mechanism to relate the central parameter of his theory, the compactivity  $X$ , to the experimentally controlled parameters such as  $\Gamma$ . Thus, in our opinion the theory is not closed. Within his formalism, it is quite a challenge to systematically compute the entropy of a disordered system. Recently, the Chicago group [14] determined  $X$  using a fluctuation formula such as eq.(7). Note, however, that this is an *experimental* method used to determine  $X$ , and a formula relating  $X$  to control parameters is still missing.

Our theory departs from Edwards in two ways: First, it is a thermodynamic theory of the *configurational statistics* of a *nonequilibrium dynamical state* or *steady state*. In this view point, the dynamics of compaction [14-15] might be viewed as a transition of an unstable state into an equilibrium state [9]. The temperature equation may be ignored in the hydrodynamic approach of the convective instability of granular materials [16,17]. Next, the relationship between the temperature variable and the control parameters was determined by comparing the *kinetics* and *thermodynamics*. This provides a closure to Edward's thermodynamic theory by providing a specific relationship between the temperature or compactivity and the external control parameters. However, the thermodynamic theory in the presence of gravity with a *hard sphere* gas presents some interesting puzzles and needs to be pursued in the future, notably the question of whether or not the temperature is an extensive quantity along the direction of anisotropy. For example, consider point particles confined in a three dimensional box of size  $(L_x, L_y, L_z)$  under gravity along the  $z$  direction, for which the energy level is given by  $\epsilon = p^2/2m + mgz$ . One can show easily that the energy per particle  $\bar{u}$  is given by

$$\bar{u} \equiv E/N = \frac{1}{N} \frac{\partial \ln Z}{\partial \beta} = \frac{5}{2} kT - f(x) \quad (8)$$

where  $Z = z^N/N!$  is the partition function of the  $N$  particle system,  $z = (2m\pi/\beta)^{3/2} L_y L_x (1 - \exp(-\beta x))/\beta mg$ , and  $f(x) = x \exp(-\beta x)/(1 - \exp(-\beta x))$  with  $x = mgL_z$ . In the limit

$L_z \rightarrow \infty$ , the energy per particle obeys the equipartition theorem and approaches  $5kT/2$ . Further it approaches zero at the zero temperature limit. Note also that the total energy  $E$  is an extensive quantity, and the thermodynamic relation between the temperature and the entropy also is satisfied, namely:  $S/k = \ln Z + \beta E$  and

$$\frac{1}{k} \frac{\partial S}{\partial E} = \frac{1}{k} \left( \frac{\partial S}{\partial \beta} \right) \left( \frac{\partial E}{\partial \beta} \right)^{-1} = \beta/k = 1/T. \quad (9)$$

However, for granular materials with finite diameter  $D$  (hard spheres), the situation becomes a little different. In the zero temperature limit, while the kinetic energy approaches zero, the potential energy is still a function of disorder and it is *not* zero. For point particles, both the kinetic and potential energy approach zero because particles can be compressed indefinitely. Further, for a hard sphere gas, the potential energy is not extensive and thus the temperature  $T$  is not intensive. Consider for example the granular materials confined in a two dimensional box of width  $L$  and the height  $H$ , for which the potential energy  $E_o = LH \frac{H}{2} = LH^2/2$ . Now, change the box size by a factor two: if the width is increased to  $2L$ , then the potential energy doubles, i.e:

$$E = 2LH \bullet \frac{H}{2} = 2E_o. \quad (10a)$$

Hence, the energy is extensive. On the other hand, if the height is increased by a factor 2, then the potential energy increases by a factor 4, i.e:

$$E = L \bullet 2H \bullet \frac{2H}{2} = 4E_o. \quad (10b)$$

So, the energy is not extensive. Hence, one finds here that while the energy does not depend on the way the system is doubled for point particles, it does for hard spheres with finite diameter. The thermodynamic definition of the temperature with hard spheres in the presence of gravity does not seem so simple as in the case of point particles. This is not inconsistent with recent experimental result [30], where it was reported that even though the velocity profiles obey perfect Gaussian, one needs two different temperatures to describe the velocity profile of excited grains in a vibrating bed

*Third*, comments can be made about the MD code which was used. It is important to note that the MD code used in this work allows the grains to deform upon contact and the amount of deformation, in particular along the normal direction, depends on the mass and the spring constant (See eq.8). Within this MD code, unlike the assumption made in the theory that particles are compact and nondeformable, the temperature does depend weakly on the *mass* of the grain. More precisely, when a spring with the spring constant  $K$  is displaced a distance  $\Delta z$  by a mass  $m$ , the velocity of the mass is given by  $\frac{1}{2}mv^2 = \frac{1}{2}K(\Delta z)^2$ , i.e.  $v = (K/m)^{1/2}$ . Now, note that in the MD code [11] used in this paper, the normal contact force at the bottom plate,  $F$ , has three components.

$$F = K_n(\Delta r)^m - mg - \gamma_n m_{eff}(\hat{v} \bullet \hat{n})$$

where the first term is the Hertzian contact force [12], the second term is the gravity term, and the third term is due to the dynamic friction. Since the acceleration of the particle,  $a$ , is given by  $a = dv/dt = F_n/m$ , and the first term is independent of the mass, the bouncing velocity of the particle at the bottom plate *is* a function of the mass for a given  $K_n$ . Therefore, the jumping height of the ball *does* depend on the mass of the particle. While the MD codes that allow such deformation are based on certain models [18] and experiments [19], it is not certain at this point whether such mass dependent dynamics of deformable grains is a realistic modeling of real granular materials. Presumably, this ambiguity might have had some effect on the discrepancies in the amplitude for the center of mass and its fluctuations. It is highly desirable to carry out the same study undertaken here with a hard sphere MD code [20] which does not allow such deformations to occur.

*Fourth*, one can discuss the problem of granular compaction and the question of surface tension. In three dimensional systems, many metastable configurations exist, which result in the hysteresis-dependent density profile as observed in the experiment of Knight et al [14]. Their experiment has shown that non-sinusoidal shaking in the form of a pulse leads to density profiles that are history dependent, with a relaxation that is logarithmic. While it is not difficult to qualitatively explain such behavior within the context of our ideal Fermi

picture [1], one should recognize the importance of *interactions* among free Fermions for the quantitative discussion of dynamical behaviors of granular particles in three dimensions. This is a challenge that must be faced in the future. It is important to point out that the temperature for granular systems has a gap at  $T=0$  which may have some interesting consequences in the excitation spectrum. Furthermore, an observation is made which is known even for hard core particles, that an effective attractive interaction exists through the direct correlation function [5]. This induces a curvature term in the free energy formulation and may be important in describing the dynamics of wet sands [29]. In the presence of such a curvature term, one of the notable predictions of the theory presented in this paper and in [1] is the existence of a dynamic surface tension [21] for excited granular materials in a vibrating bed. At this point, the existence of the curvature term in the free energy seems to be at variance with recent experiments conducted by several groups[22] on surface fluidization. In these experiments, the dispersion relation for the excited surface waves in shallow vibrating beds seems to be consistent with that in deep water without any capillary corrections. While the authors do not doubt the correctness of the experimental results, it is certain that more careful studies are needed on the question of surface tension of granular materials, in particular, dynamic surface tension, both theoretically and experimentally.

*Fifth*, one of the conceptually important issues is to rigorously examine the theoretical basis of the view presented above (and hence improve or correct) that the driven nonequilibrium dissipative system might be viewed as a thermodynamic equilibrium state, if one stays focused on configurational statistics. In the problem of pattern formation, such as the selection problem of dendrites[23] and viscous fingers [24], the free energy approach is of no value. However, it has been shown experimentally that statistically averaged profiles of patterns in the fractal viscous fingering problem reduces to the zero surface tension solution of the Saffman-Taylor problem.[25] Here, one sees a similar example of the existence of non-trivial configurational statistics and its relation to the steady state patterns. Perhaps, the study of the vibrating bed of granular materials along the direction outlined above, namely

the thermodynamic approach to nonequilibrium systems, may provide some clues to such questions. We also point out that the microscopic basis of the Fermi statistics has been recently examined by one of the authors in ref. [26], where it was demonstrated that the crossover from Boltzmann to Fermi statistics as the vibrational strength decreases arises via the condensation of granular particles under gravity [26]. This is another consequence of the excluded volume interaction of finite grains that one cannot compress such a system indefinitely, which is the key to uncovering an interesting phenomena of 'condensation of grains under gravity. Putting aside the mathematical aspect of this condensation, which is *mathematically* similar to Bose condensation, the underlying physics of this phenomenon is not difficult to understand. If we start with particles at a high temperature and decrease the temperature slowly, then a portion of particles begins to settle down from the bottom, and two phases develop: a fluidized region near the top and a solid or glass region near the bottom. This is what we term the condensation phenomenon of granular particles, and in the presence of such two phases, the continuum theory may pose some problems. For detailed summary of how the kinetic theory describes such a condensation phenomenon, see ref.[26].

Finally, granular materials as hard core Bosons. The observation of Fermi statistics [1] and condensation [26] of granular materials may appear to be contradictory at first glance in view of the Pauli exclusion principle of spinless Fermions and the nature of Bosons. Such can be resolved, however, if one may view the grains as hard core Bosons. For example, by a suitable transformation(i.e. the Wigner-Jordan transformation [27]), one may transform the Boson Hamiltonian into that of a Fermion in a magnetic field. Note that in such a formulation, the spin variable is not really relevant. The condensation of hard core Bosons discussed in [26] may reflect the validity of such an approach and the excitation spectrum of such Fermions may lead to a theory similar to Fermi liquid theory, and thereby the results known for Fermi systems in a magnetic field may be probed with granular materials, if proper Hamiltonians are chosen. This is an interesting challenge in the future. Further, one may introduce internal variables that may resemble spins for grains. The so called q-

model of Coppersmith [28] that takes into account grain contacts may be an ideal choice for extending our theory along this direction. Such an internal variable may be important in granular dynamics.

## Acknowledgement

We wish to thank many people for their assistance during the course of this project, especially J. Lee for providing us with the Molecular Dynamics code, and S. Luding for many valuable suggestions on the subtle aspect of MD simulations. We also wish to thank H. Hayakawa for constructive criticisms and comments over the course of this work, as well as M.Y Choi for comments on the thermodynamics of point particles with gravity and the hard core nature of grains.

## References

- [1] H. Hayakawa and D. C. Hong, Phys. Rev. Lett. **78**, 2764 (1997)
- [2] E. Clement and J. Rajchenbach, Europhys. Lett. **16**, 1333 (1991)
- [3] For the parking lot analogy in slow relaxation of polymer absorption problem, see E. Ben-Naim, J. Chem. Phys. **100**, 6778 (1994) and ref.[14].
- [4] See., eg., T.L. Hill. *Statistical Mechanics* (Dover, New York, 1987), Chapt.8.
- [5] S. Warr and J. P. Hansen, Euro. Phys. Lett. Vol. 36, no.8 (1996)
- [6] J.P. Hansen and I. R. McDonalds, *Theory of Simple Liquids*, Academic Press, London (1986); See also, G. Ristow, Phys. Rev. Lett. **79**, 833 (1997).
- [7] H. Caram and D. C. Hong, Phys. Rev. Lett. **67**, 828 (1991).
- [8] J. Litwiniszyn, Bull. Acad. Polon. Sci., Ser. Sci. Tech. **11**, 61 (1963); See also, W.W. Mullins, J. Appl. Phys. **43**, 665 (1972); *ibid* J. Appl. Mech. 867 (1974)
- [9] H. Hayakawa and D. C. Hong, Int. J. Bifurcations and Chaos, Vol.7, 1159 (1997)
- [10] J.M. Luck and A. Mehta, Phys. Rev. E **48**, 3988 (1993)
- [11] See for example: J.A.C. Galls, H. Herrmann, and S. Sokolowski, Physica(Amsterdam) **189A**, 437 (1992), G.H.Ristow, G. Strassburger, and I. Rehberg Phys. Rev. Lett. **79**, 833 (1997); For hard sphere MD codes, see: S. Luding, 'Models and simulations of granular materials,' Ph.D. thesis, Albert-Ludwigs University, Germany (1994); See also; S. Luding, H. J. Herrmann, and A. Blumen, Phys. Rev. E **50**, 3100 (1994); T. Schwagar and T. Poeschel, cond-matt/9711313; S. McNamara and W. Young, Phys. Fluids. A4 (3), 496 (1992)
- [12] See for example, *Contact Mechanics*, K.L. Johnson, Cambridge University Press (1985)
- [13] S.F. Edwards and R.B.S. Oakeshott, Physica A **157**, 1080 (1989); A. Mehta and S.F. Edwards, Physica A(Amsterdam) **168**, 714 (1990) For other thermodynamic theories of grains, see: B. Bernu, F. Deylon, and R. Dazighi, Phys. Rev. E **50**, 4551 (1994); J.J.Brey,

F. Moreno, and J.W. Duffy, Phys. Rev. E **54**, 445 (1996)

[14] J.B.Knight, C.G. Fandrich, C.N. Lai, H.M. Jaeger, and S. R. Nagel, Phys. Rev. E **51**, 3957 (1995); E. Nowak, J. Knight, E. Ben-Naim, H.M. Jaeger, and S.R. Nagel, *Density Fluctuations in Vibrated Granular Materials*, Preprint;

[15] G. Barker and A. Mehta, Phys. Rev. E **47**, 184 (1993); D.C. Hong et al, Phys. Rev. E **50**, 4123 (1994); E. Caglioti, V. Loreto, H. J. Herrmann, and M. Nicodemi, Phys. Rev. Lett. **79**, 1575 (1997)

[16] M. Bourzutschky and J. Miller, Phys. Rev. Lett. **74**, 2216(1995); H. Hayakawa, S. Yue and D. C. Hong, Phys. Rev. Lett. **75**, 2328 (1995); P. Haff, J. Fluid. Mech. **134**, 401 (1986); J.T.Jenkins and S.B. Savage, J. Fluid Mech. **130**; C. Saluena and T. Poeschel, cond-mat/9807071; 187 (1983); K. Aoki et al, Phys. Rev. E., **54**, 874 (1998); Y-h. Taguchi, Phys. Rev. Lett. **69**, 1367 (1992); J. Gallas, H. Herrmann, and S. Sokolowski, *ibid*, **69**, 1371 (1992); D.C. Hong and S.Yue, Phys. Rev. E **58**, 4763 (1998)

[17] P. Evesque and J. Rajchenbach, Phys. Rev. Lett. **62**, 44 (1989); E. Clement, J. Duran, and J. Rajchenbach, Phys. Rev. Lett. **69**, 1189 (1992); Y-h. Taguchi, Europhys. Lett. **24**, 203(1993); K. Ichiki and H. Hayakawa, Phys. Rev. E **52**, 658 (1995); H.K.Pak and R. Behringer, Nature(London) **371**, 231(1994); S. Daoudy, S. Fauve, and C. Laroche, Europhys. Lett. **8**, 621 (1989).

[18] H. Brandt, J. Appl. Mech. Vol.22, 479 (1955); Deresiewicz, *ibid*, Vol.25, 402 (1958); P. J. Digby, *ibid* Vol.48, 803 (1981)

[19] S. Forester, M. Louge, H. Chang, and K. Allia, Phys. Fluids. **6** (3), 1108 (1994)

[20] Jysoo Lee, cond-mat/9606013; S. Luding, E. Clement, A. Blumen, J. Rajchenbach, and J. Durna, Phys. Rev. E. **50** R1762 (1994)

[21] For example: S. Safran, *Statistical Thermodynamics of Surfaces, Interfaces, and Membranes*, Addison-Wesley (1994) Chapter 2.

[22] F. Melo, P. Umbanhowar, and H. Swinney, Phys. Rev. Lett. **72**, 172 (1994); Phys. Rev. Lett. **75**, 3838 (1995); E. Clement, J. Duran, and J. Rajchenbach, Phys. Rev. Lett. **69**, 1189 (1992); S. Luding, E. Clement, A. Blumen, J. Rajchenbach, & J. Duran, Phys. Rev. E **50** 4113 (1994)

[23] J.S. Langer, Science **243**, 1150 (1989) and references therein; D. Kessler, J. Koplik, and H. Levine, Adv. Phys. **37**, 255 (1988); *Dynamics of Curved Fronts*, edited by P. Pelce (Academic, New York, 1986); M. Ben-Amar and Y. Pomeau, Euro. Phys. Lett. **2**, 307 (1986); P. Pelce and Y. Pomeau, Stud. Appl. Math. **74**, 245 (1986); A. Barbieri, D.C. Hong, and J. S. Langer, Phys. Rev. A **35**, 1802 (1987)

[24] B. Schraiman, Phys. Rev. Lett. **56**, 2028 (1986); R. Combescot, T. Dombre, V. Hakim, Y. Pomeau, and A. Pumir, *ibid*, **56**, 2033 (1986); D.C. Hong and J.S. Langer, *ibid*, **56**, 2032 (1986); Phys. Rev. A **36**, 2325 (1987);

[25] A. Arnerdo, F. Argoul, Y. Couder, & M. Rabaud, Phys. Rev. Lett. **66** 2332 (1991)

[26] D. C. Hong, “Condensation of hard spheres under gravity,” Cond-matt/9806253.

[27] See for example; E. Fradkin, Field theories of condensed matter systems, Addison-Wesley, 1991

[28] S. Coppersmith et al, Phys. Rev. E. 53, 4673 (1996)

[29] D. Hornbaker, R. Albert, I. Albert, A.L. Barabasi, and P. Schiffer, Nature, Vol 387, 765 (1997)

[30] J. Delour, A. Kudrolli, J. Gollub, Velocity distribution in a vertically vibrated granular media, cond-matt/980-6366.

## Figure Captions

Fig.1. Density profile for  $\Gamma = 20$ (square) and  $\Gamma = 2$ (circle) with  $N=100$  and  $\Omega = 4$ . For  $\Gamma = 2$ , the inequality eq.(3) that insures the validity of the Fermi statistics is satisfied. The Fermi statistics breaks down for  $\Gamma = 20$  and the density profile is approaches that of the dilute gas with gravity, shown with the dashed line.

Fig.2 Density profiles for different  $\Gamma$  's are plotted for (a)  $N=100$ ,  $\Omega = 4$ , (b)  $N=200$ ,  $\Omega = 4$ , (c)  $N=200$ ,  $\Omega = 8$ , (d)  $N=100$ ,  $\Omega = 4$ ,  $\Gamma = 2.0$ , (e)  $N=200$ ,  $\Omega = 4$ ,  $\Gamma = 2.0$ , (f)  $N=200$ ,  $\Omega = 8$ ,  $\Gamma = 2.0$ . The solid lines are the fittings with the Fermi profile (eq.(2)).

Fig.3. The log-log plot of the scaling of the measured temperature,  $T$ , against the controlled parameters (a) frequency -  $\omega$ , (b) gravity -  $g$ , and (c) the diameter -  $D$ . The solid lines are a guide for the eye and their slopes are: 1.167( $\omega$ ), 0.48( $g$ ) and 0.528( $D$ ) respectively.

Fig.4 The center of mass,  $\langle z(T) \rangle$ , is plotted for  $N=100$   $\Omega = 4$  and  $N=200$   $\Omega = 4$  for both the sine wave and triangle wave vibration and  $N=200$   $\Omega = 8$  for the sine wave vibration as a function of  $T^2$ . The straight lines are a guide to the eye.

Fig.5. Fluctuations in the center of mass,  $\langle (\Delta z(T))^2 \rangle$ , is plotted for  $N=100$   $\Omega = 4$  and  $N=200$   $\Omega = 4$  for both the sine wave and triangle wave vibration and  $N=200$   $\Omega = 8$  for the sine wave vibration as a function of  $T^3$ . The straight line is a guide to the eye.

## Table Captions

Table I. The dimensionless maximum jump height,  $H_o(\Gamma)$ , of a single ball launched gently at the vibrating plate as a function of the vibration strength  $\Gamma$ . The best fit is:  $H_o(\Gamma) = -0.192079 \bullet \Gamma^3 + 2.063404 \bullet \Gamma^2 - 2.093293 \bullet \Gamma$ .

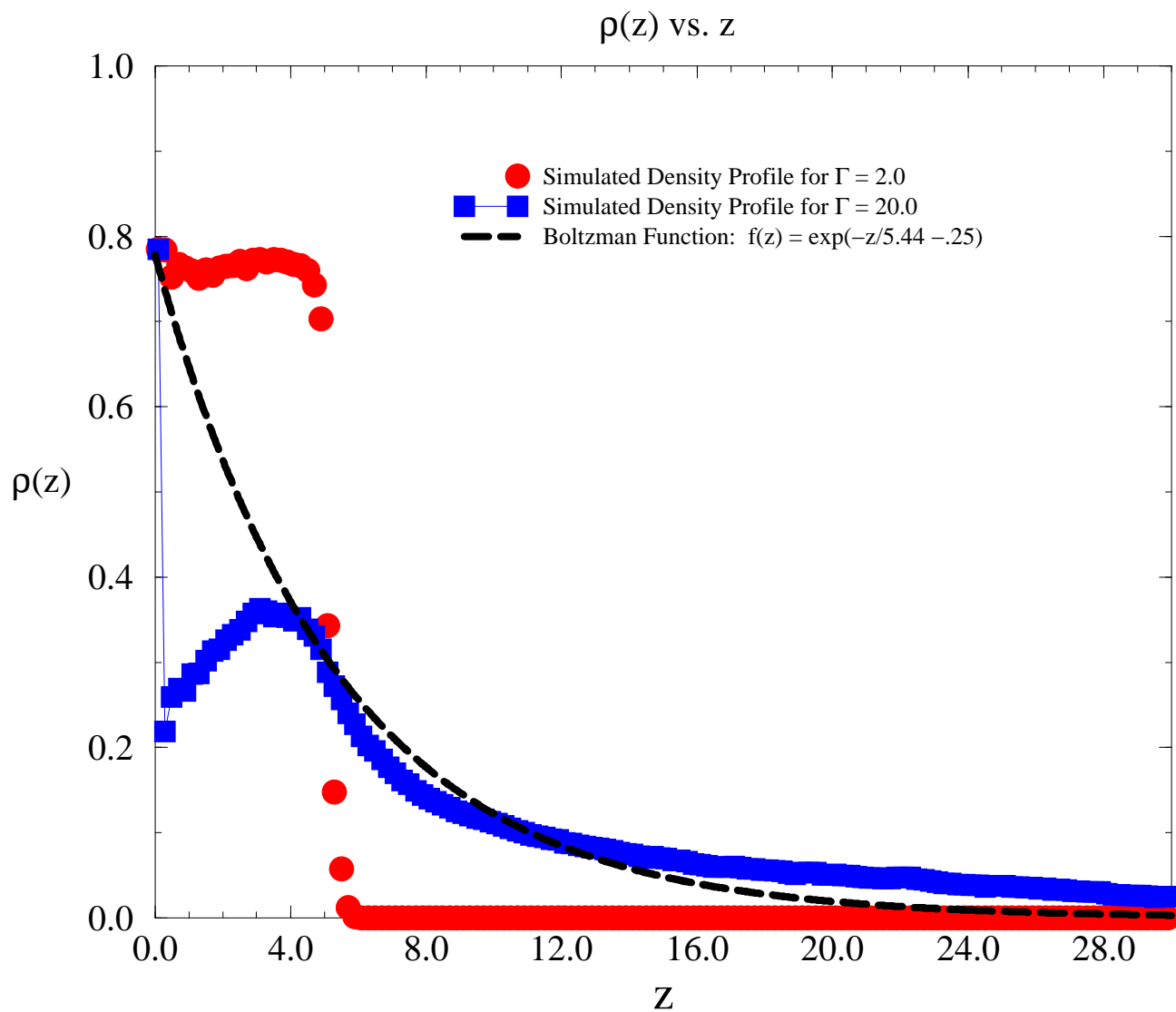
Table II. A set of parameters used in the simulations with a sine wave vibration for various  $\Gamma$  for  $N=100$   $\Omega = 4$ ,  $N=200$   $\Omega = 4$ , and  $N=200$   $\Omega = 8$ . Initially, particles are arranged in a square lattice. Here,  $\Gamma$  is the vibration strength,  $\rho_c$  is the density of the system before the vibration,  $\mu$  is the Fermi energy,  $A$  is the amplitude of the vibrations,  $D$  is the diameter of the particle, and  $R = \Gamma A/D \gg 1$  is the condition for the validity of the Fermi statistics.(See Eq.(3)).

Table III. The temperature,  $T_{fit}$ , determined for  $N=100$   $\Omega = 4$ ,  $N=200$   $\Omega = 4$ , and  $N=200$ ,  $\Omega = 8$  under a sine wave vibration. The  $T$ 's are the predicted ones (Eq.(6a)-(6b)).

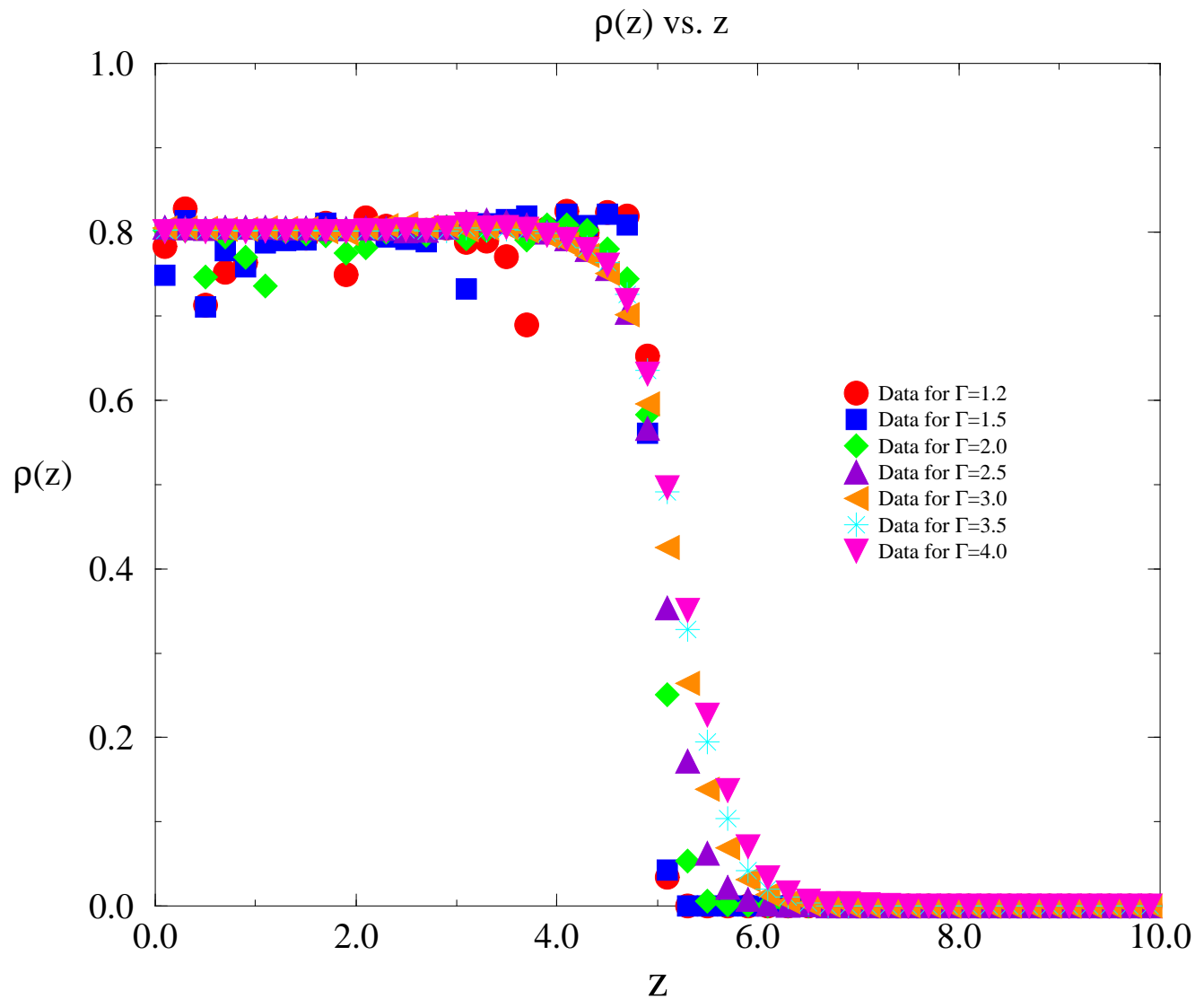
Table IV. A set of parameters used in the simulations with a triangle wave vibration for various  $\Gamma$  for  $N=100$   $\Omega = 4$  and  $N=200$   $\Omega = 4$ . Initially, particles are arranged in a square lattice. Here,  $\Gamma$  is the vibration strength,  $\rho_c$  is the density of the system before the vibration,  $\mu$  is the Fermi energy,  $A$  is the amplitude of the vibrations,  $D$  is the diameter of the particle, and  $R = \mu\Gamma A/D \gg 1$  is the condition for the validity of the Fermi statistics.(See Eq.(3)).

Table V. The temperature,  $T_{fit}$ , determined for  $N=100$   $\Omega = 4$ ,  $N=200$   $\Omega = 4$ , and  $N=200$ ,  $\Omega = 8$  under a triangle wave vibration. This  $T[(h_o \max(\Gamma))]$  is the predicted one Eq.(6b).

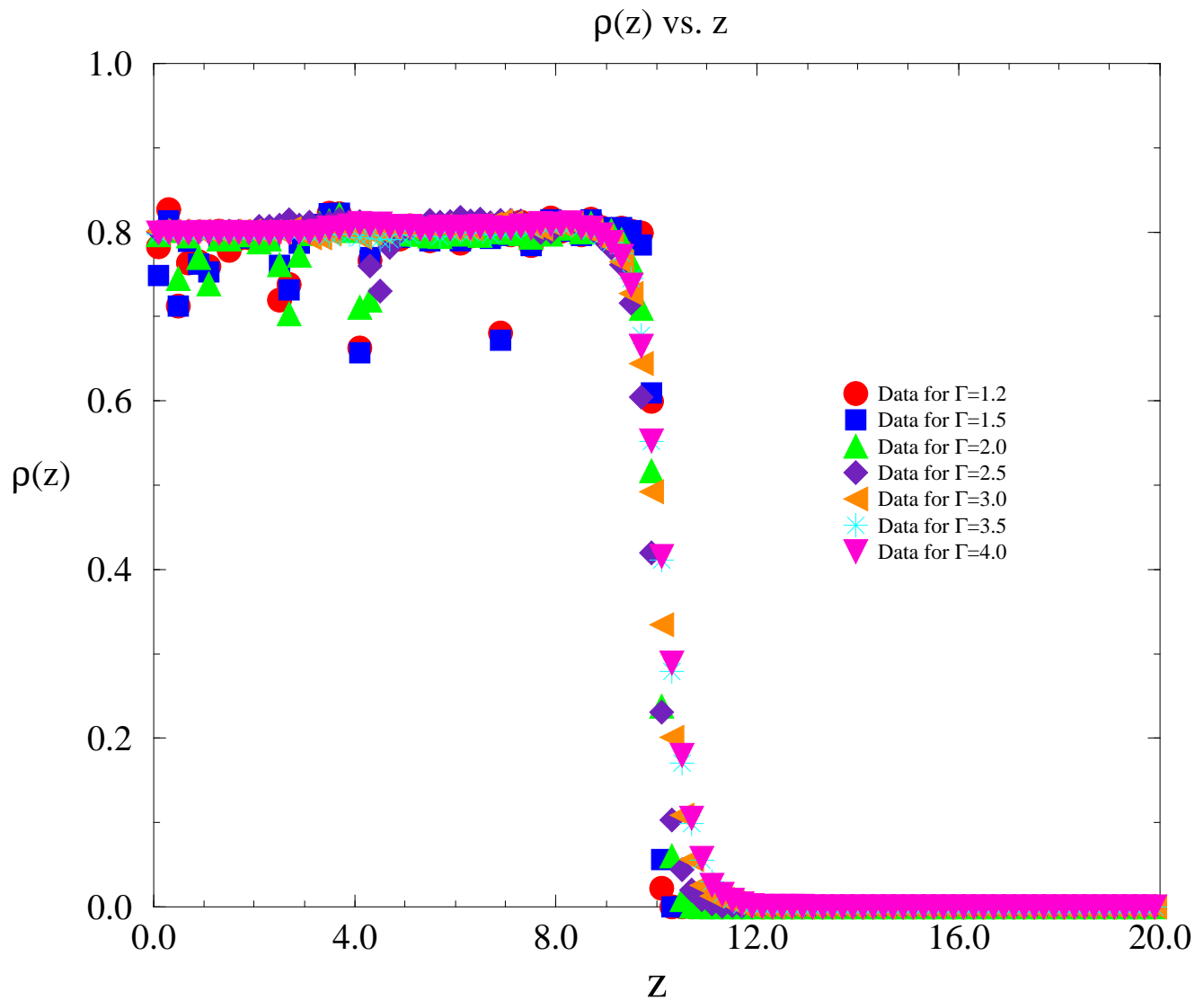
# Density Profile for 100 Particles, $\Omega=4$ , $\Gamma=2.0$ and $\Gamma=20.0$



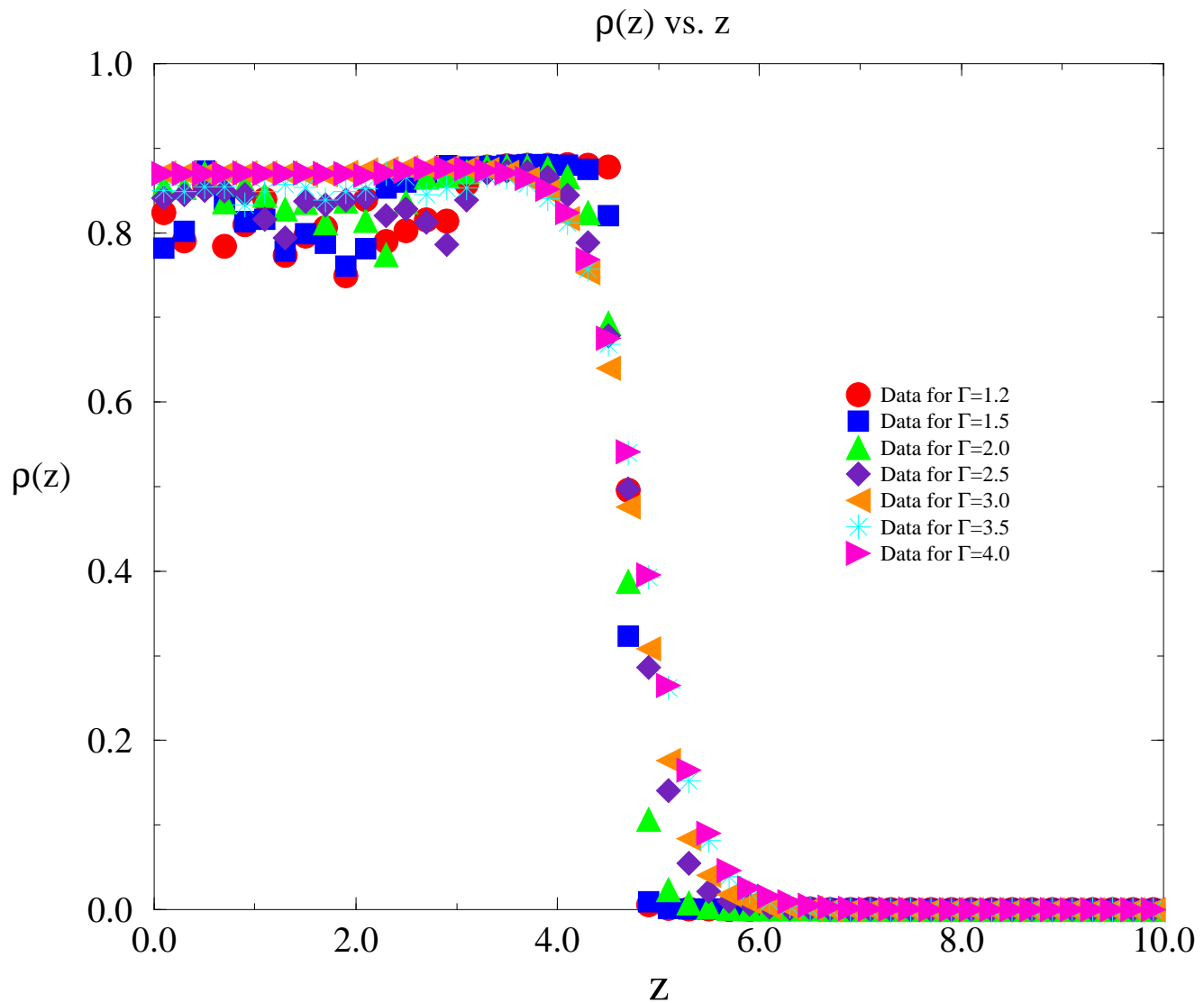
# Density Profiles for 100 Particles, $\Omega=4$



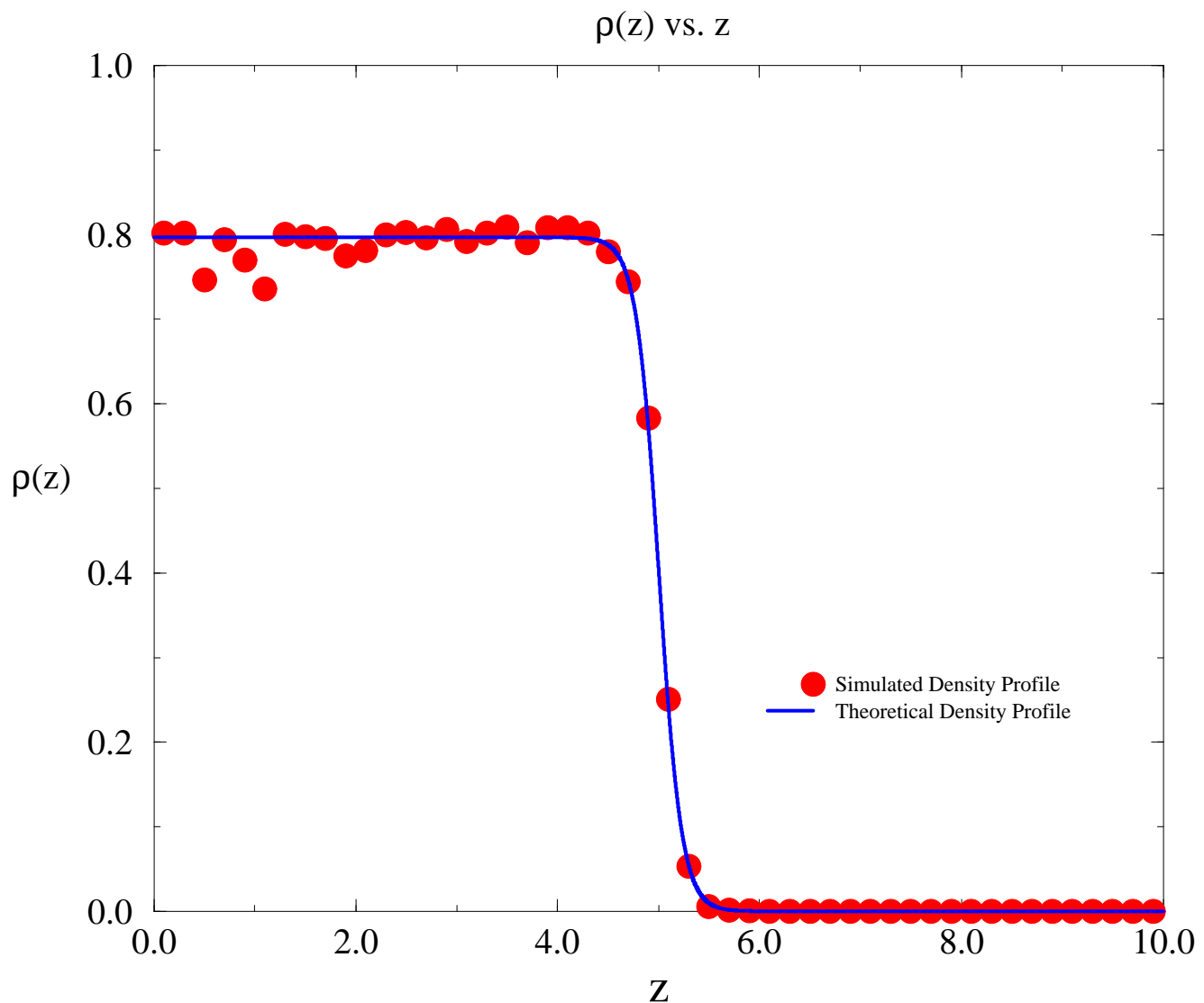
# Density Profiles for 200 Particles, $\Omega=4$



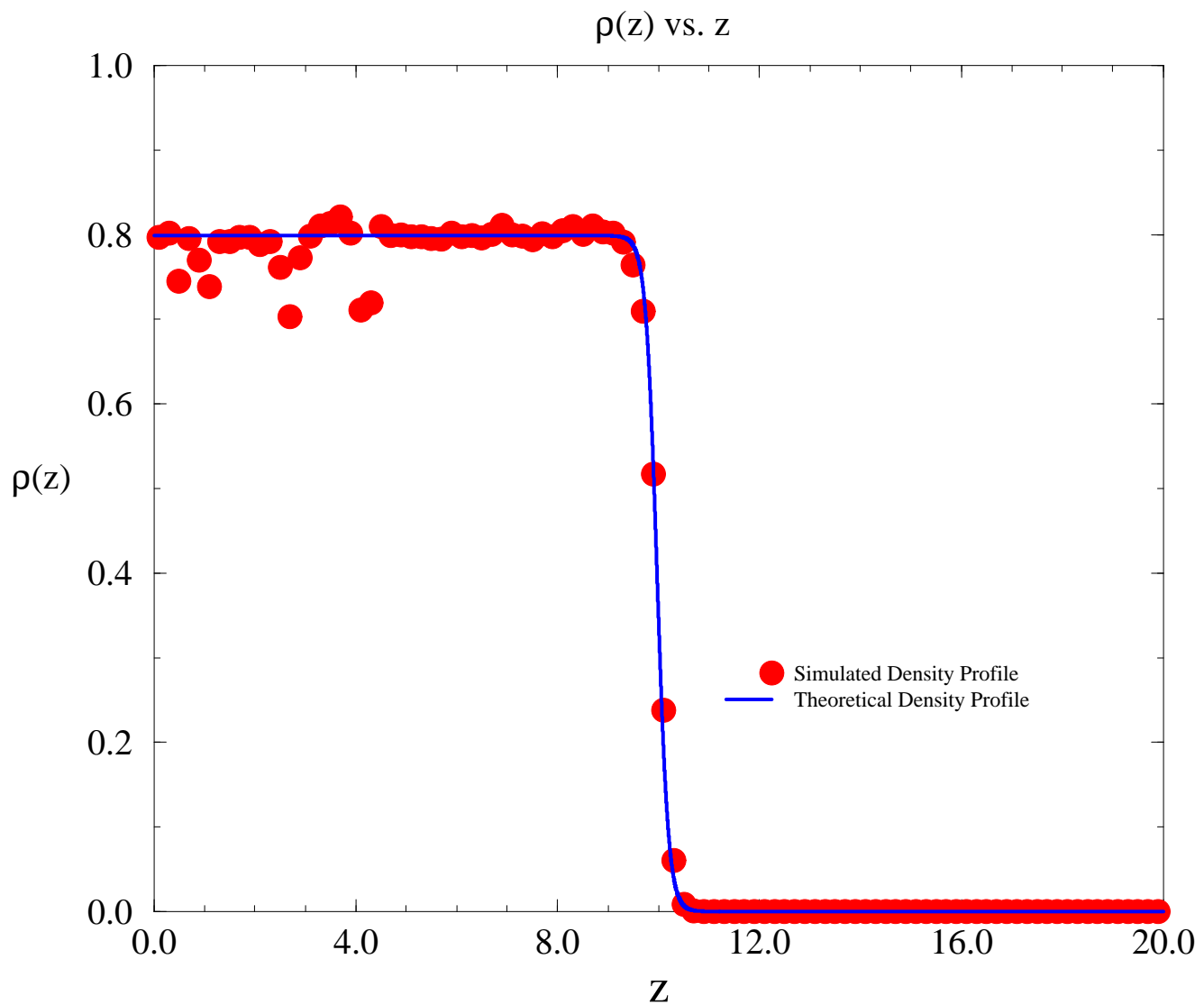
# Density Profiles for 200 Particles, $\Omega=8$



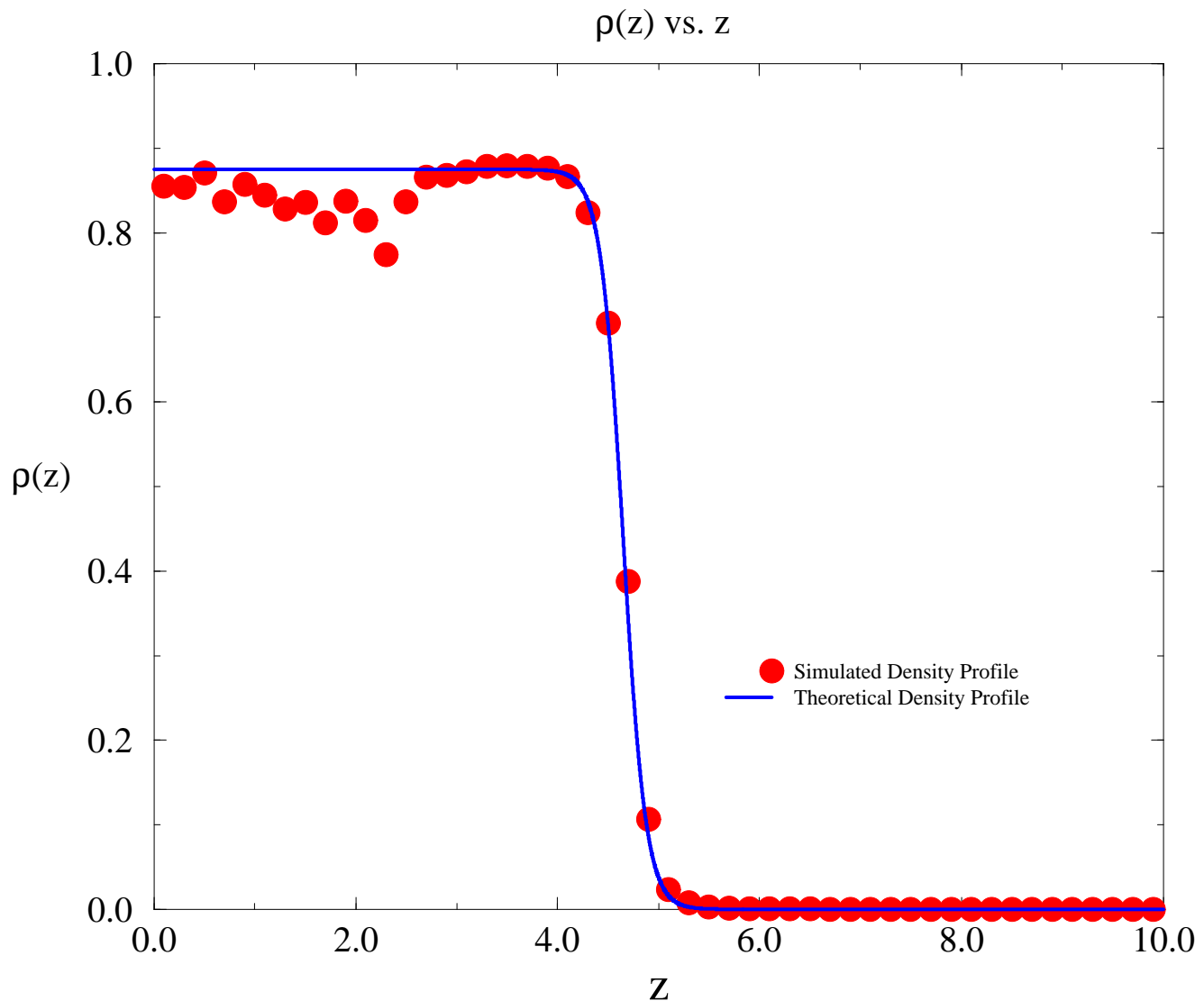
# Density Profile for 100 Particles, $\Omega=4$ , $\Gamma=2.0$



# Density Profile for 200 Particles, $\Omega=4$ , $\Gamma=2.0$

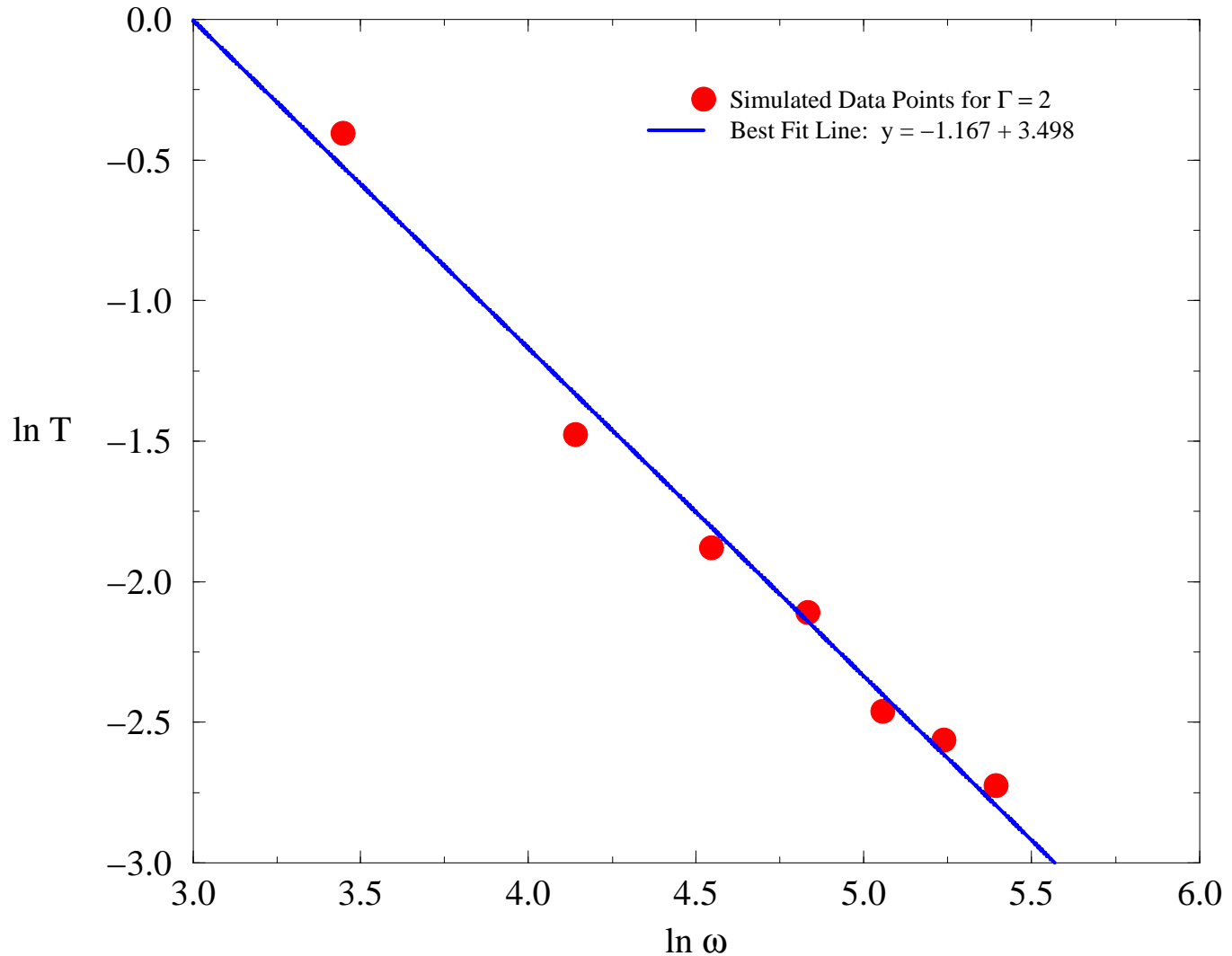


# Density Profile for 200 Particles, $\Omega=8$ , $\Gamma=2.0$



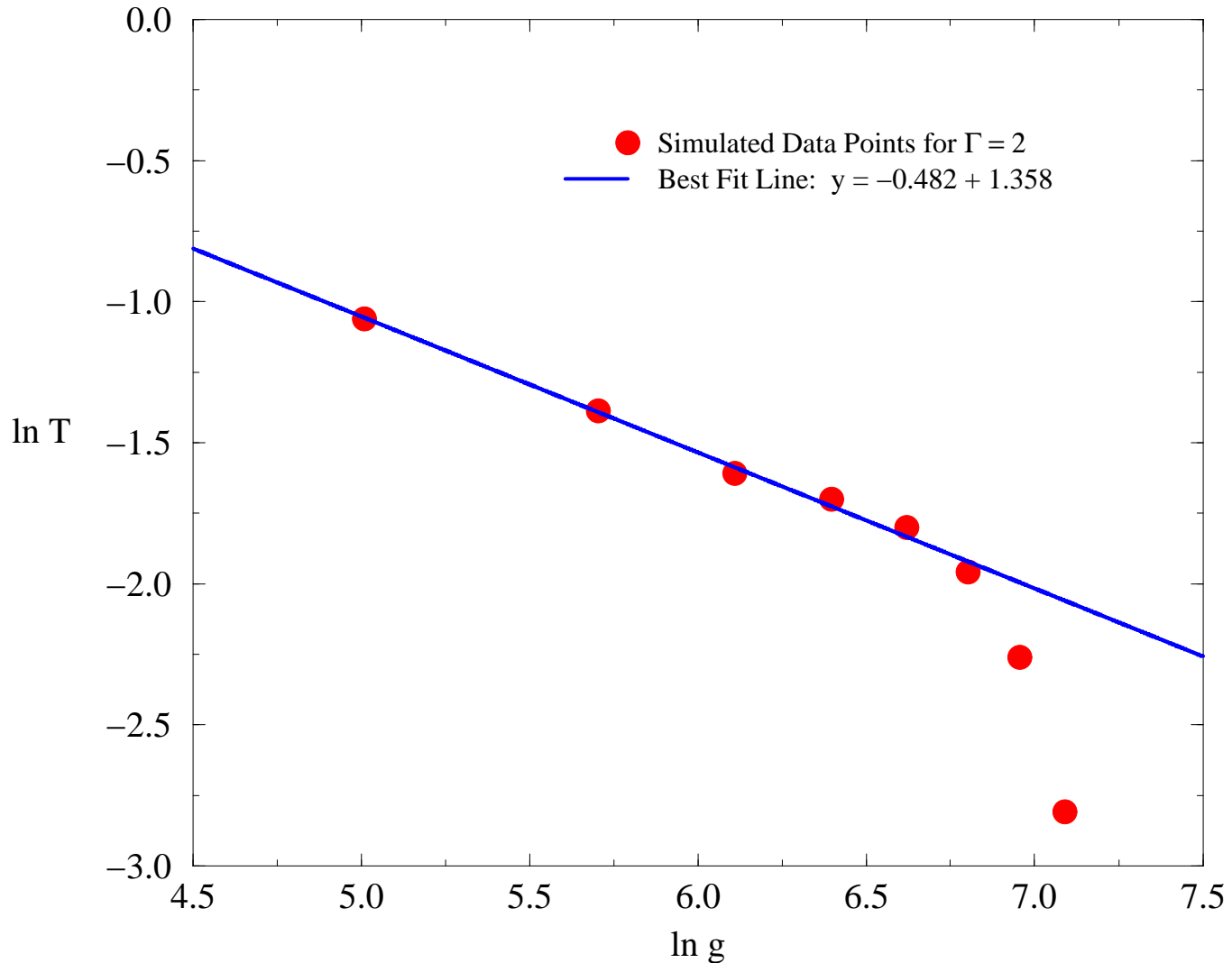
# Power Relationship Between T and $\omega$

Ln T vs. Ln  $\omega$



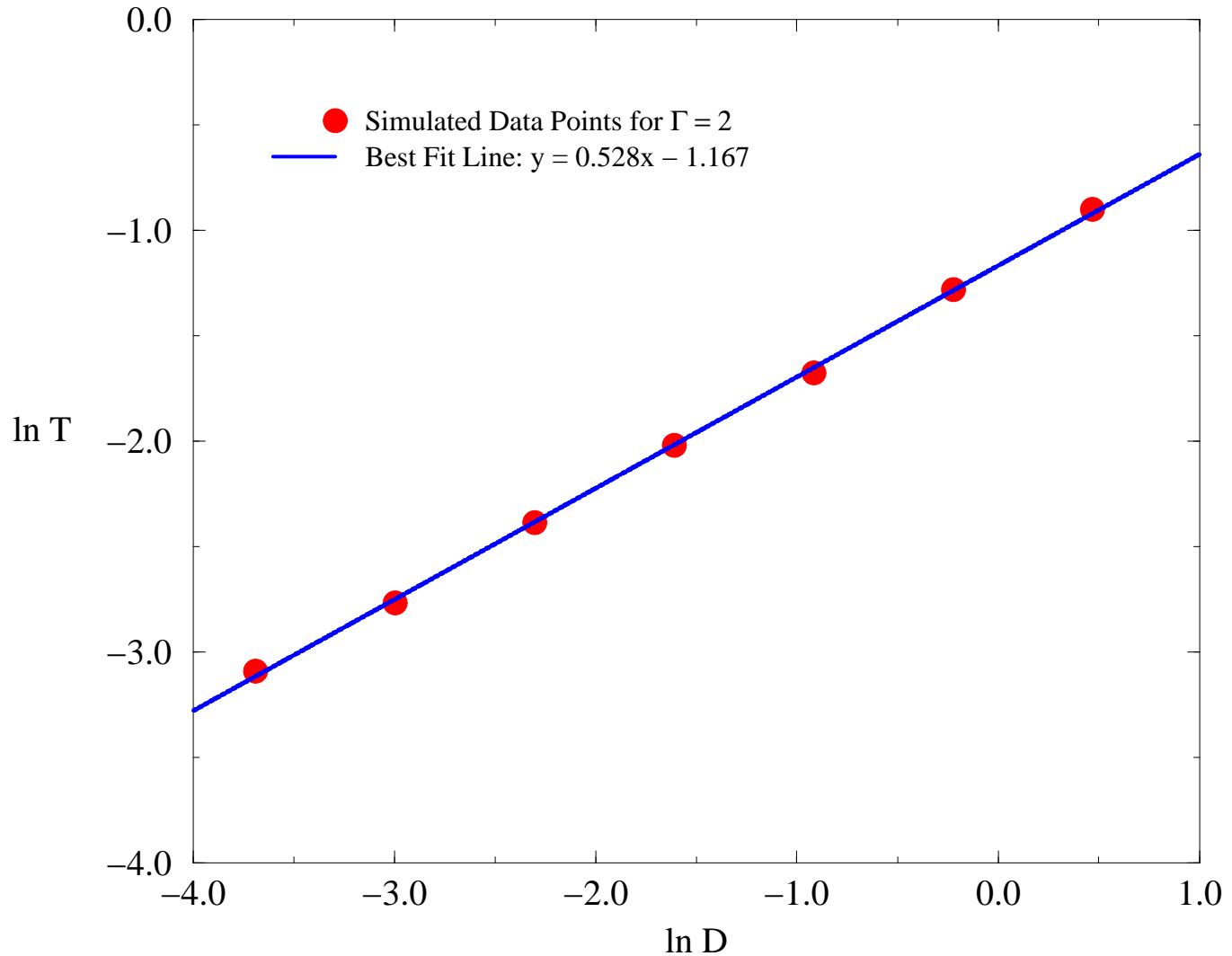
# Power Relationship Between T and g

Ln T vs. Ln g



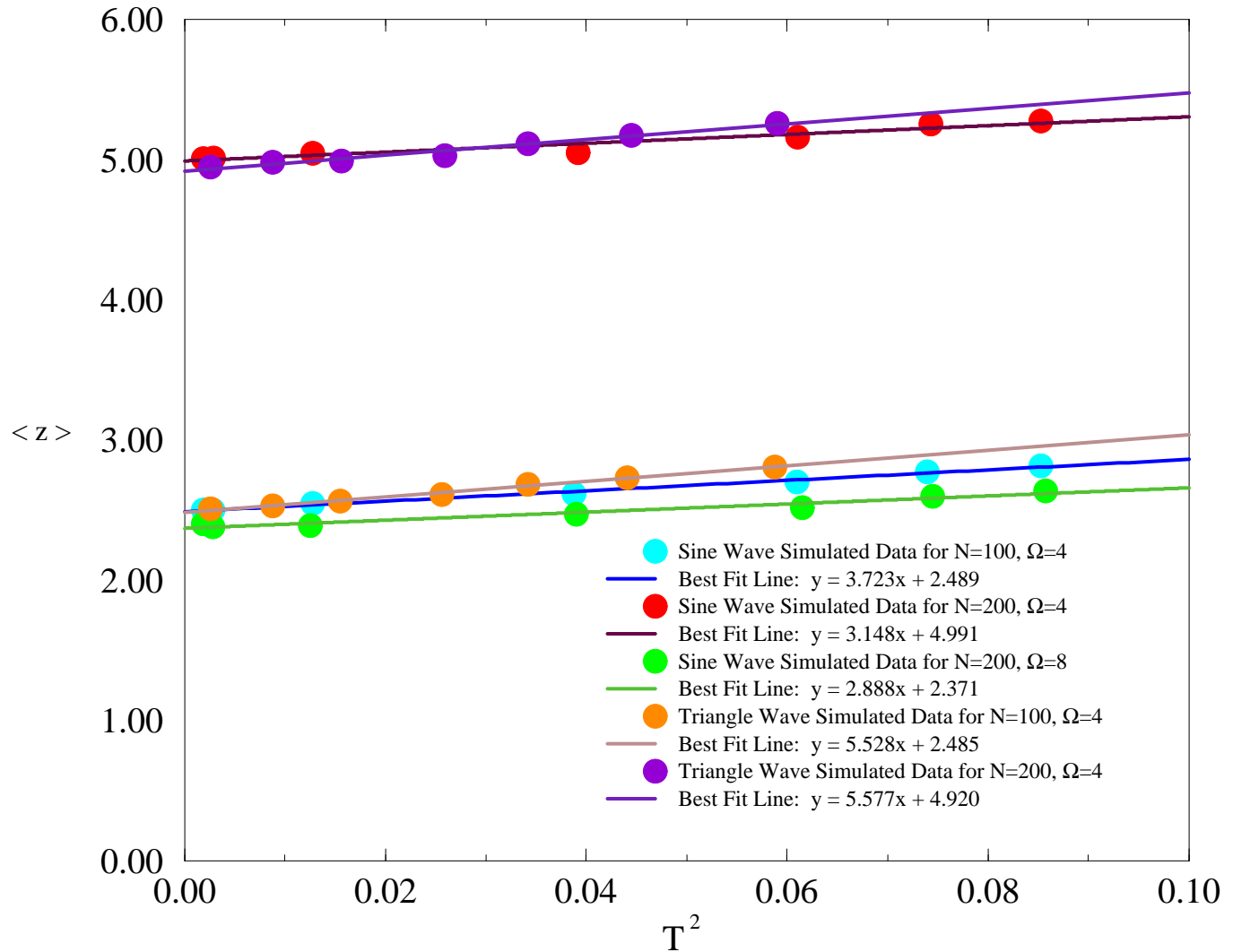
# Power Relationship Between T and D

Ln T vs. Ln D

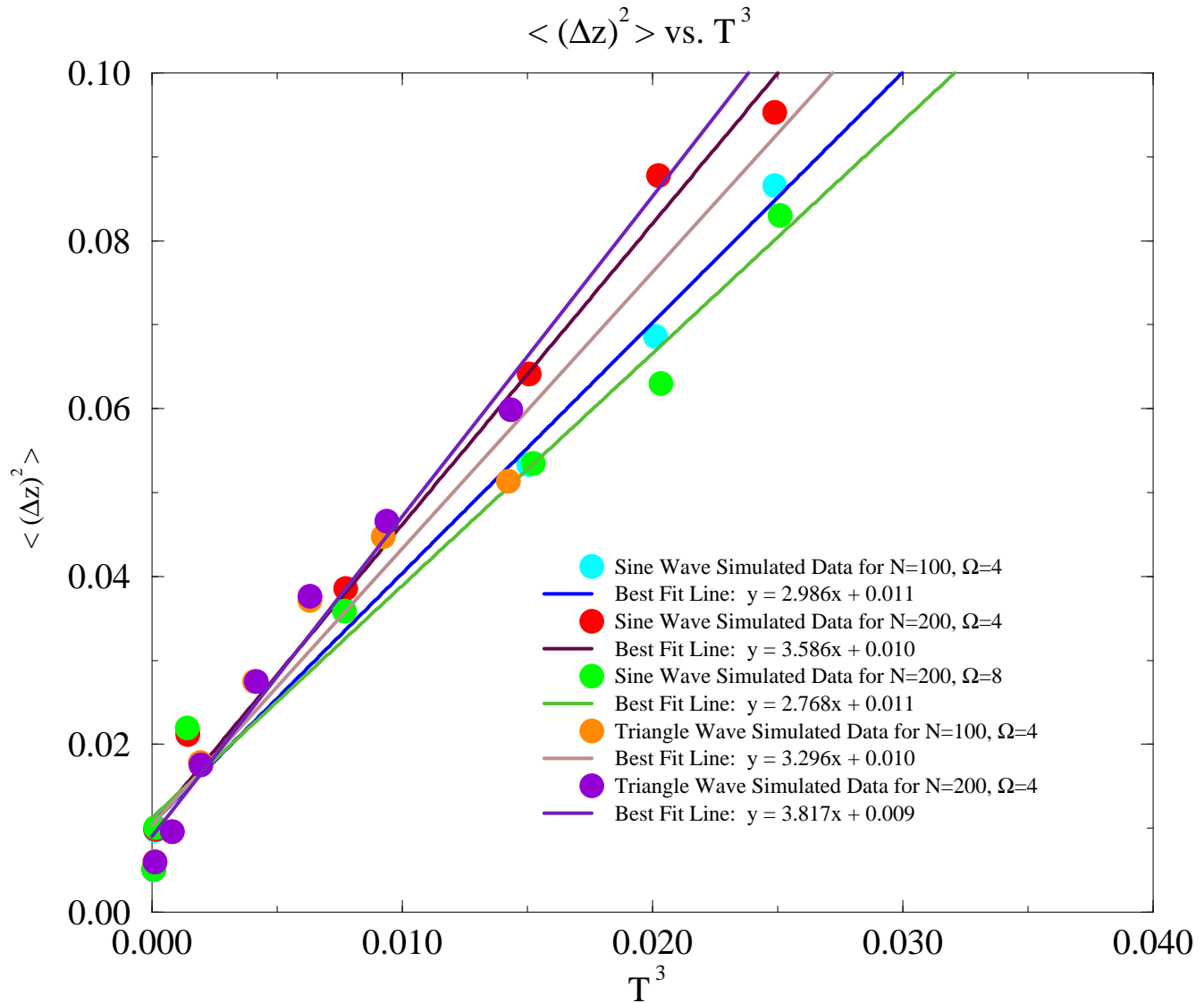


# 100 Particles, $\Omega=4$ and 200 Particles, $\Omega=4$ and $\Omega=8$

$\langle z \rangle$  vs.  $T^2$



# 100 Particles, $\Omega=4$ and 200 Particles, $\Omega=4$ and $\Omega=8$



$\Gamma$	$H_o(\Gamma)$
1.2	0.155337
1.5	0.807449
2.0	2.531511
2.5	4.694872
3.0	7.108747
3.5	9.681423
4.0	12.362321

$\Gamma$	A	N = 100, $\Omega = 4$			N = 200, $\Omega = 4$			N = 200, $\Omega = 8$		
		$\rho_c$	$\mu$	R	$\rho_c$	$\mu$	R	$\rho_c$	$\mu$	R
1.2	0.07455	0.81	4.96	55.45	0.80	9.95	111.20	0.81	4.73	52.05
1.5	0.09318	0.82	4.94	35.35	0.80	9.94	71.25	0.88	4.71	33.70
2.0	0.12425	0.80	5.00	20.07	0.80	9.97	40.10	0.88	4.65	18.71
2.5	0.15531	0.81	5.06	13.05	0.81	9.91	25.51	0.87	4.76	12.25
3.0	0.18637	0.80	5.13	9.20	0.81	10.03	17.95	0.88	4.75	8.50
3.5	0.21743	0.81	5.22	6.85	0.80	10.13	13.32	0.87	4.86	6.39
4.0	0.24849	0.81	5.24	5.25	0.81	10.13	10.20	0.88	4.87	4.90

$\Gamma$	Fitting Temperature, $T_{fit}$			$T[h_o max(\Gamma)]$	$T[H_o(\Gamma)]$
	N=100, $\Omega = 4$	N=200, $\Omega = 4$	N=200, $\Omega = 4$		
1.2	0.04324	0.04300	0.04300	0.05497	0.03424
1.5	0.06100	0.06999	0.06000	0.09404	0.08105
2.0	0.13000	0.13999	0.13500	0.14598	0.13821
2.5	0.19700	0.19799	0.19759	0.19701	0.18822
3.0	0.25000	0.25100	0.25999	0.25443	0.23161
3.5	0.26000	0.26500	0.26999	0.26471	0.27028
4.0	0.30100	0.30100	0.30500	0.31664	0.30541

$\Gamma$	A	N = 100, $\Omega = 4$			N = 200, $\Omega = 4$		
		$\rho_c$	$\mu$	R	$\rho_c$	$\mu$	R
1.2	0.07455	0.80	4.96	55.45	0.80	9.81	109.65
1.5	0.09318	0.80	4.98	35.65	0.80	9.86	70.50
2.0	0.12425	0.80	5.00	20.07	0.80	9.86	39.58
2.5	0.15531	0.80	5.05	12.95	0.80	9.88	25.45
3.0	0.18637	0.80	5.14	9.20	0.80	9.97	17.85
3.5	0.21743	0.81	5.16	6.80	0.81	10.01	13.15
4.0	0.24849	0.80	5.26	5.29	0.80	10.15	10.20

$\Gamma$	Fitting Temperature, $T_{fit}$		$T[h_o max(\Gamma)]$
	N=100, $\Omega = 4$		N=200, $\Omega = 4$
1.2	0.06500	0.06000	0.08366
1.5	0.09361	0.09360	0.09040
2.0	0.12464	0.12499	0.12739
2.5	0.15265	0.15999	0.15159
3.0	0.19259	0.19000	0.19275
3.5	0.21000	0.21099	0.21373
4.0	0.24225	0.22499	0.24579